Holocene landscape evolution in the Baza Basin (SE-Spain) as indicated by fluvial dynamics of the Galera River

D Wolf, F J García-Tortosa, C Richter, Julie Dabkowski, C B Roettig, D Faust

Quaternary Science Advances 4 (2021) 100030

Contents lists available at ScienceDirect

Quaternary Science Advances

journal homepage: www.sciencedirect.com/journal/quaternary-science-advances

Holocene landscape evolution in the Baza Basin (SE-Spain) as indicated by fluvial dynamics of the Galera River

D. Wolf [a,*], F.J. García-Tortosa [b], C. Richter [a], J. Dabkowski [c], C.B. Roettig [a], D. Faust [a]

[a] Technische Universität Dresden, Helmholtzstr. 10, 01069, Dresden, Germany
[b] Universidad de Jaén, Campus Las Lagunillas, 23071, Jaén, Spain
[c] CNRS, Laboratoire de Géographie Physique: environnements quaternaires et actuels (UMR 8591 Paris 1 Panthéon-Sorbonne, UPEC), 1 place A. Briand, FR-92195, Meudon CEDEX, France

ARTICLE INFO

Keywords:
Western mediterranean
Granada geopark
Quaternary
Tufa deposits
River incision
Divergence phenomenon

ABSTRACT

The concrete relationships between fluvial system behavior and potential influencing factors that are, among others, climate forcing, tectonics, and human activity are a key issue in geomorphological research. In this regard, especially the Iberian Peninsula is an area of great interest because its landscapes are highly sensitive towards climate changes and anthropogenic impact. Nowadays, the Iberian Peninsula reveals a strongly heterogeneous and spatially fragmented climate configuration. This should give rise to disparate behavior of fluvial geomorphic systems considering that climate is generally assumed the most important trigger of fluvial dynamics. In fact, river systems located in more humid and more arid regions in Iberia often reveal deviating patterns of Holocene floodplain evolution. This raises the question of whether these patterns were actually caused by a different climate history or if, alternatively, other factors might have been responsible. In this study, we investigated the Holocene floodplain evolution of the Galera River that is located in the upland of Eastern Andalucía (SE-Spain) named Baza Basin. A combination of detailed stratigraphic profile logging and close-meshed radiocarbon dating revealed that Holocene river dynamics generally followed the regional climatic development, which proves the Galera floodplain record to be a valuable archive of Holocene landscape evolution. However, we demonstrate that fluvial dynamics of the Galera system are hardly comparable to other river systems in Iberia even if the climate evolution was not so different. Our results suggest that in river systems with different basic conditions and catchment-specific configurations, similar climatic influences may lead to deviating fluvial process regimes (divergence phenomenon) because of substantial imprints of other parameters such as geological substratum, relief composition, tectonics, or human interventions.

1. Introduction

Today as in the past, the Iberian Peninsula reveals highly heterogeneous climate and environmental conditions demonstrating strong spatial variations (Vicente-Serrano et al., 2006; Queralt et al., 2009; Hidalgo-Muñoz et al., 2011; Pérez-Obiol et al., 2011; Lillios et al., 2016; Tarroso et al., 2016; Morellón et al., 2018). This means that climate relevant data in high spatial resolution is needed for reconstructing and understanding underlying mechanisms of the climate system and resulting earth surface dynamics. The most humid parts of the Iberian Peninsula exhibit generally good preservation conditions for environmental archives and are therefore often linked to a higher spatial density of palaeoenvironmental information (e.g. Martínez-Cortizas et al., 2009; Carrión et al., 2010). In contrast, arid to semiarid zones such as the Guadix-Baza-Basin (GBB) in SE-Spain show a certain paucity in terrestrial archives providing continuous records for the Holocene period. In such regions, a strong natural pressure on ecosystems originated from recurring drought periods during the Holocene (Carrión et al., 2003; Gil-Romera et al., 2010; Bellin et al., 2013) that were massively reinforced by human land use measures starting as early as 5 ka cal BP (Carrión et al., 2010) or even earlier (Carrión et al., 2007). The millennia lasting impact of both droughts and degradation due to human land use resulted in progressive deforestation and large-scale erosion dynamics (Bellin et al., 2011; García-Alix et al., 2013) that even led to the formation of badlands in different areas (Torri et al., 2000; Nadal-Romero and García-Ruiz, 2018). In these strongly dissected landscapes,

* Corresponding author. TU Dresden, Institute of Geography, Helmholtzstr. 10, 01069, Dresden, Germany.
E-mail address: daniel_wolf@tu-dresden.de (D. Wolf).

https://doi.org/10.1016/j.qsa.2021.100030
Received 29 March 2021; Accepted 12 May 2021
Available online 18 May 2021

environmental archives are largely absent and mostly limited to adjacent mountain regions (e.g. Carrión, 2002, 2007; Anderson et al., 2011; Mesa-Fernández et al., 2018) or cave records (e.g. Carrión et al., 1999; Budsky et al., 2019). From this follows that there is a high demand for studies of climate-sensitive terrestrial archives in order to understand past climate dynamics and predict future system changes due to global warming, especially in these dry regions in SE-Iberia.

Remedy may arise from fluvial sediment sequences in floodplain areas that represent palaeoenvironmental archives with an almost ubiquitous distribution even in the dry areas of semiarid and arid SE-Iberia. Owing to their relief positions, floodplain deposits are less affected by surface erosion. Moreover, they generally provide a clear indication of landscape evolution within the catchment (Wolf and Faust, 2015). The great value of floodplain deposits for palaeoenvironmental reconstructions has been shown in many cases (Blum and Törnqvist, 2000; Macklin et al., 2012), also on the Iberian Peninsula (e.g. Schulte, 2002; Benito et al., 2008; Carmona and Ruiz, 2011; Wolf and Faust, 2015). However, several aspects should be considered before interpreting floodplain records in terms of climatic conditions (see review by Faust and Wolf, 2017). As a prerequisite, a reliable standard stratigraphy is based on a number of profile sections that help identifying common sedimentation patterns as well as singularities. Furthermore, an appropriate age model is based on a cautious handling of sufficient dating realized on material suitable for avoiding age-overestimation. Finally, a reliable interpretation requires an ample consideration of characteristics of the river catchment since every fluvial system has a never-recurring individuality. This is related to the non-repetitive spatial constellation of a catchment area, which always varies greatly in terms of size, relief configuration, basic geological structure and tectonic features, geomorphological diversity, precipitation and runoff regime, connectivity of sub-systems, vegetation dynamics and land-use history (Antoine et al., 2000; Vandenberghe, 2003; Faust and Wolf, 2017).

Based on excellent outcrop conditions, the floodplain of the Galera River turned out to be an outstanding palaeoenvironmental archive for studying Holocene landscape evolution within the Baza Basin (Fig. 1) that we consider to be of supra-regional importance even beyond SE-Spain. In order to exploit this floodplain record and in view of the above-mentioned suggestions, this study encompasses the following objectives.

(1) A standard stratigraphy will be derived based on eight individual profile sections;
(2) a highly resolved chronology will be based on extensive radiocarbon dating;
(3) a critical evaluation of the results will be realized against the background of detailed catchment analyses for providing a reliable record for climate and environmental reconstruction.

2. Geographical setting

The Galera River is located in the heartland of the recently established UNESCO-Geopark of Granada (Fig. 1). It is a tributary to the Guardal River named downstream Guadiana Menor River. The Guadiana Menor River is the main river of a huge river network draining the

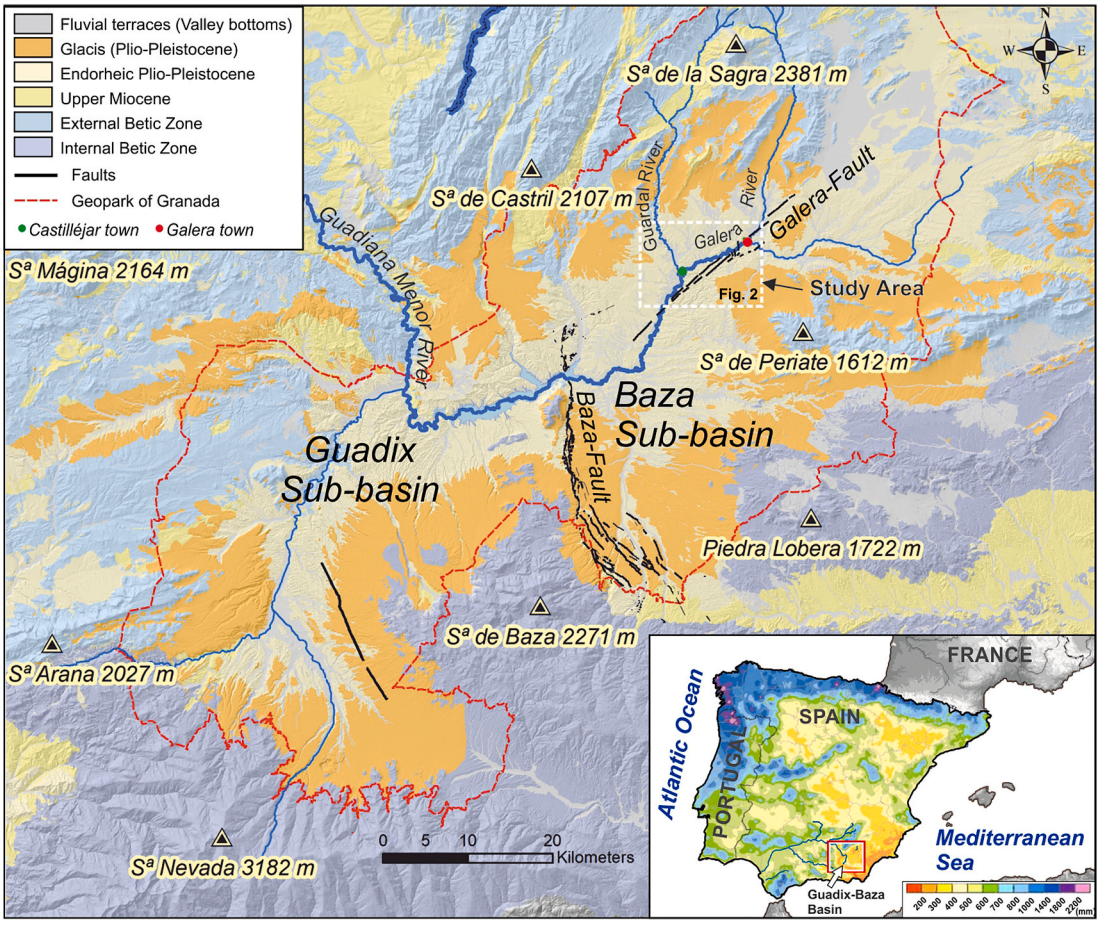

Fig. 1. Map of the study area within the Baza Basin (eastern part of Guadix-Baza Basin) with indication of geomorphological and lithological units. The Galera river system is generally a sub-catchment of the Guadalquivir Basin, but due to its position within the eastern Andalusian uplands, it climatically belongs already to the drier southeastern part of Iberia. The lower right inset shows the general situation of the Guadix-Baza Basin (GBB) in Iberia. Moreover, mean values of annual precipitation are shown (adapted from Iberian Climate Atlas, 2011).

Guadix-Baza Basin (GBB). The Baza Sub-basin is situated in the eastern part of the GBB that is the largest of the late Neogene inland basins of the Betic Cordillera (Gibert et al., 2007). It is delimited by the Sierra de Cazorla, Sierra de Castril, Sierra Seca y Sierra de la Sagra in the north and by a couple of mountain ranges (Sierra de Baza, Sierra de los Filabres, Sierra de Lucar, Sierra de Orce, Sierra de Maria) in the south and south-east (Fig. 1). While Triassic metamorphic rocks dominate the southern mountains, the northern ranges are mainly composed of Jurassic and Cretaceous limestone, dolomites and marls. The Baza Sub-basin itself was filled with up to 2.000–3.000 m thick lacustrine sediments since the late Miocene (Alfaro et al., 2008). Along the lower Galera River with an elevation of about 830 m a.s.l., the basin infill is characterized by early Quaternary deposits such as limestone and white calcareous sandstone as well as gypsiferous marl that was evaporated in the former center of the depression (Peña, 1985; García-Aguilar et al., 2014).

The relief configuration in the study area is dominantly determined by the dissection of the basin infill by the fluvial drainage network. The date of fluvial capture of the GBB by the Guadalquivir river system (transition from endorheic to exorheic conditions) and thus, the beginning of the incision of the fluvial network is a widely debated issue. Scientific assumptions for the time of this capture range between the early to mid-Quaternary (Gibert et al., 2007; Scott et al., 2007; García-Tortosa et al. 2008a, 2008b) until the late Quaternary (Ortiz et al., 2004; García-Tortosa et al. 2008a, 2008b, 2008b; Perez-Peña et al., 2009; Oms et al., 2011) period. However, incision should have started before 220 ka according to dating of the Alicún de las Torres travertine formation in the western part of the GBB (Prado-Pérez et al., 2013). The progress of fluvial dissection as well as the fluvial sedimentation history of the Baza Basin have hardly been investigated so far. The recent Galera river channel is cut about 100 m deep into the surface of the formerly endorheic glacis. A couple of different Pleistocene fluvial terrace levels are observable in the study area that were not systematically mapped or dated yet. The youngest valley fill and terraces that relate to the Holocene period are the research objects of this study (Fig. 2).

Tectonic development played an important role for the depositional conditions during the endorheic phase (Haberland et al., 2017; Gibert et al., 2007; García-Aguilar et al., 2013) and also determines erosional processes in the subsequent exorheic phase (García-Tortosa et al., 2011). The widespread GBB is divided into an elevated western part and a relatively sunken eastern sub-basin by the north-south trending Baza Fault (Fig. 1) (García-Tortosa, 2008; García-Tortosa et al., 2011).

The study area is characterized by a cold semiarid steppic climate with a mean annual precipitation of 423 mm and an average annual temperature of 14.4 °C in recent times. However, a marked seasonality prevails with cold and moist winters (monthly mean of 5 °C and ~45 mm prec.) and hot and dry summers (monthly mean of 24 °C and ~6 mm prec.). Based on anthracological studies, Rodríguez-Ariza (1992) found that semiarid meso-mediterranean plant associations and especially dense kermes oak woods (*Quercus coccifera*) would dominate the natural vegetation in the area, while gypsum substrates would be characterized by a mosaic of oak groves, Aleppo pines (*Pinus halepensis*), and tree-less areas. Floodplain areas and valley floors are nowadays intensely used for agriculture. The potential natural vegetation has been strongly modified due to human land use during the middle to late Holocene period. In combination with the soft and highly erodible substrate, this turned the central Baza Sub-Basin into a strongly dissected landscape that is highly vulnerable to the effects of erosion processes and sediment relocation. According to archaeological findings, the Galera river catchment was intensively used for agricultural purposes already 4.1 ka ago in the course of the El-Algar culture (Lull et al., 2013) when oak woods and pine forests were cleared for cultivation purposes (Rodríguez-Ariza, 1992). Latest 2.5 to 2.1 ka ago with the onset of the Iberian Period, vegetation types reached a predominantly unnatural state with a large increase of cereal production that reduced natural vegetation to smaller occurrences of degraded shrubs ('matorrales').

3. Methods

3.1. Field-work

The main effort of this study relates to fieldwork and profile descriptions. In a first phase, an up to 13 m high terrace body was identified and mapped all over the study area. This terrace takes up large parts of the recent valley floor and shows a very characteristic

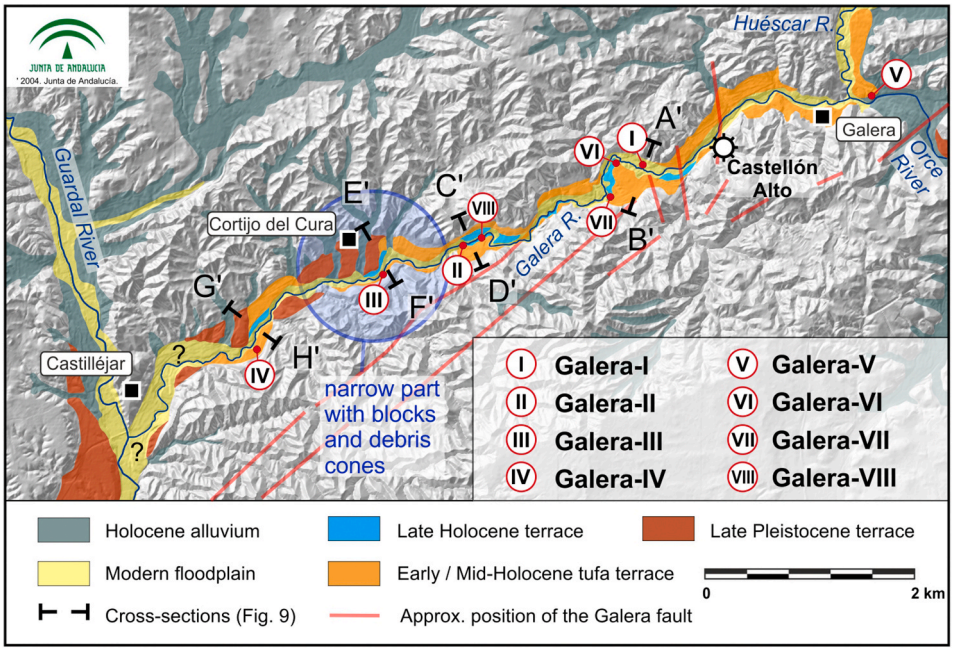

Fig. 2. Location of the study area with indication of studied sections. Lettering indicates cross-sections shown in Fig. 9. The blue circle marks the narrow passage of the Holocene floodplain around Cortijo del Cura that is accompanied by large collapsed boulders and debris cones. The lowermost part of the Galera floodplain close by Castilléjar (question marks) was not mapped because of lacking outcrops and limited access.

appearance including a thick sequence of fluvial tufa deposits. The geological substratum that frames the valley of the Galera River is composed of laminated calcareous and gypseous marl deposits with thin blackish layers containing clay and lignite (Gibert et al., 2007). These layers assumedly refer to a high phytoplankton productivity and anoxic conditions during formation times (García-Aguilar et al., 2014). With this appearance, the late Pliocene/early Quaternary lacustrine (endorheic) deposits look somewhat similar to the Holocene fluvial and alluvial deposits, but are, on closer examination, clearly distinguishable by a more compacted and consolidated character as well as a plethora of well-formed gypsum crystals. In the lower stretch of the Galera River, the Holocene terrace body slowly merges into an erosional terrace that was carved from the marl substratum and that shows nearly the same elevation like the surface of the Holocene deposits. Thus, a careful mapping was indispensable for gathering a reliable distribution of Holocene deposits in the study area. Wide areas of the Galera Valley between the towns of Galera and Castilléjar (Fig. 2) were vastly shaped by the construction of cultivated field terraces that often mask the real distribution of fluvial terraces and produced substantial erosion unconformities within the sedimentary sections. Sites with a proven occurrence of Holocene deposits were surveyed with a GPS device forming the basis for the map in Fig. 2. Eight profile sections were studied (Fig. 3) at suitable locations (in terms of accessibility and completeness of the sections) between Galera and Castilléjar (Fig. 2). Profile logging included the differentiation of sedimentary units and soil horizons, and the documentation of colors, textures, sediment structures, as well as fossil remnants such as gastropod shells, leaf imprints and root channels.

3.2. Analytical work

The profile sections GA-I, GA-II. GA-IV and GA-VIII (Fig. 3) were sampled for lab analyses in order to gain an overview of general sediment characteristics and soil forming intensities. Sampling was oriented towards sedimentary units and palaeosol horizons for obtaining a representative dataset for all sedimentary units.

Several analyses were realized in the laboratory of the Department of Physical Geography at the Technische Universität Dresden, Germany: i) Texture analyses were conducted by pipette method after Köhn and wet sieve techniques (Schlichting et al., 1995) after dispersing with sodium pyrophosphate. Because the samples contained certain quantities of gypsum that disrupted the settling process in the sample cylinder by flocculation, all samples passed through a repeated cycle of dissolution and centrifugation until measured electrical conductivity fell below a value of 400 $\mu S\,cm^{-3}$ (Frenkel et al., 1986). Considering the high contents of calcium carbonate, selected samples were measured twice in order to analyze e.g., the share of silicate clay fraction against the content of clay-sized carbonates. One run was implemented without decalcification, another run was realized after carbonates were dissolved by using 10% HCl. In addition, the electrical conductivity was used as a further evidence for the presence of soluble salts (primarily gypsum). ii) Soil organic matter was measured via suspension and catalytic oxidation (TOC-VCPN/DIN ISO 16904). iii) Carbonate content was determined by measuring the carbon dioxide gas volume after adding hydrochloric acid in a Scheibler apparatus (Schlichting et al., 1995).

3.3. Radiocarbon dating

For assessing the temporal resolution of different sedimentation and stability periods, radiocarbon dating was carried out on 29 samples of *insitu* and reworked charcoal fragments and 1 sample of a gastropod shell. The measurements on the charcoal samples were performed by the AMS ^{14}C laboratory in Miami (Beta, United States), and the shell sample was measured in the GNS Science Center in Lower Hutt, New Zealand. The age model of the Galera River sediment record was compiled based on Bayesian age modeling using the software OxCal 4.3.2 (Bronk Ramsey, 2017) with the IntCaL 13 calibration curve (Reimer et al., 2013). The mean of the 2σ probability interval is denoted in Table 1, while the implementation of the chronostratigraphic correlation is provided in chapter 4.3.

4. Results and interpretations

4.1. Stratigraphic characterization of the Galera floodplain record

The accumulation of Holocene deposits in the Galera Valley followed a prior period of severe river incision. This incision was linked to a deepening of more than 10 m according to the vertical distance between fluvial terrace remains of presumably late Pleistocene river gravels (SU-1) and lowest Holocene deposits at the valley bottom. Since datable material is largely absent from these gravels, age estimation for the beginning of the incision period is not available yet. The Holocene deposits cover consolidated early-to mid-Quaternary endorheic basement rocks with lacustrine facies. Apart from SU-7 and SU-10 that relate to colluvial deposits, all other Holocene sediment units refer to a fluvial origin.

SU-2: The base of the Holocene sequence is formed by fluvial deposits up to 8 m thick that are characterized by alternating sandy and loamy layers (Fig. 4B) with sandy layers referring to sand contents of more than 50 percent (Fig. 5). Above coarse sands and gravels (section GA-VII, Fig. 3), fine laminated clayey and silty laminae (e.g. sections GA-I, GA-III, GA-VII) indicate the presence of surface rinsing (Fig. 4F). In other parts of this unit, coarse-grained channel-fills evidence strong channel activity including erosion and sedimentation processes (see section GA-1, Fig. 5). Analytical results point to low organic carbon contents (0.1–0.4 percent) without any hints for periods of surface stability and soil formation. Calcium carbonate contents between 40 and 50 percent (Figs. 5 and 6) reflect the widespread occurrence of carbonate rocks within the closer catchment area. However, sand contents of more than 30 percent after decalcification show a long transport within the river channel as sands assumedly originated from Palaeozoic units of the framing mountain ranges. An interesting finding belongs to the two-fold realization of texture analysis, once with and once without prior decalcification (Fig. 5). While the sand fraction contains still high proportions of silicate minerals, the major part of the clay content, that rises up to more than 40 percent, consists of carbonate. This clearly illustrates that clay contents should be interpreted in terms of sedimentation processes rather than pedogenesis.

In various depths of SU-2, concentrations of discrete charcoal fragments evidence high fire activity with short distance relocation of charred materials. As a further peculiarity, micro-scale folding structures (few centimeters in diameter) resulted from the effect of seismic activities on water-saturated cohesive floodplain sediments (photograph in Fig. 4F). The whole unit is characterized by hydromorphic features, including leached segments, iron stains and strips as well as massive iron precipitations caused by aerenchym-roots that provide oxygen in anaerobe conditions.

SU-3: This unit reflects a slowdown of fluvial sedimentation dynamics. It consists of a couple of clayey sediment layers that alternate with thin sand layers, together forming a succession of fining-up sequences (section GA-I, Fig. 5). In general, more than 80 percent of the contained clay consists of calcium carbonate. There are plenty of charcoal fragments included in this unit as well as many iron-coated root channels (see photograph in Fig. 4C, lower part). The deposits of SU-3 demonstrate an appearance of typical high-flood deposits, while a slight increase of the organic content may suggest incipient soil formation processes linked to certain surface stability (see section GA-III, Fig. 3). In certain sections (e.g. GA-II), the upper part of SU-3 already intermeshes with relocated or *in situ* tufa deposits.

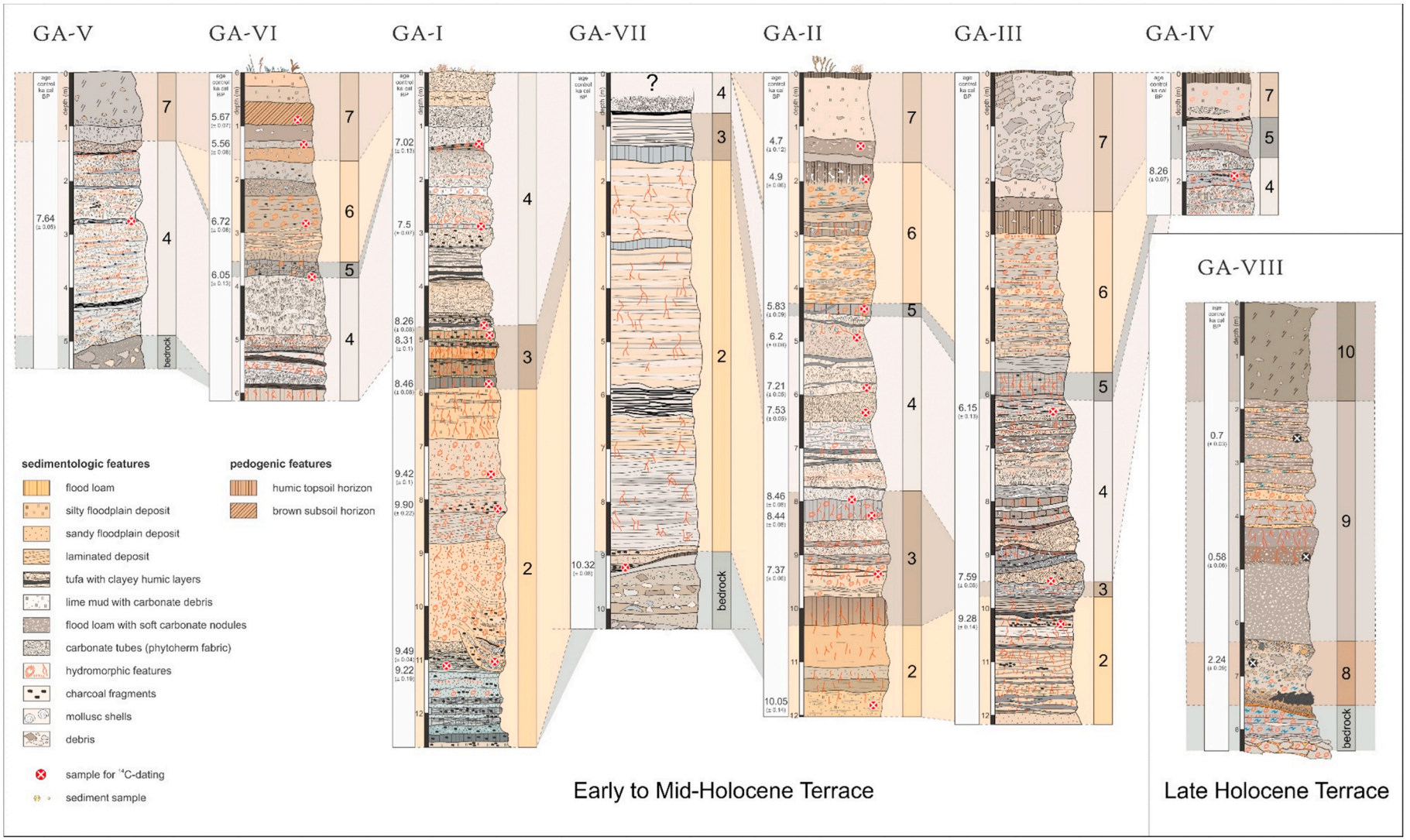

Fig. 3. Stratigraphic correlation of all profile sections indicated in Fig. 2. Visible are stratigraphic sketches, differentiation of sediment units, as well as chronological information.

Table 1
Analytical data for radiocarbon dating obtained from the Galera River system: Sample codes, material characteristics, radiocarbon ages and mean of the calibrated ages, significance of the date, and respective sediment unit.

Profile	Lab no.	Material	^{14}C age yrs BP	Calibrated age BP (2σ)	Significance	Sediment unit
GA-I	Beta-404764	charred material	6100 ± 30	7020 ± 130	active formation	SU-4
GA-I	Beta-485046	charred material	6580 ± 30	7495 ± 66	active formation	SU-4
GA-I	Beta-404762	charred material	7420 ± 30	8258 ± 78	start formation	SU-4
GA-I	Beta-485045	charred material	7530 ± 40	8311 ± 100	stagnant sedimentation	SU-3
GA-I	Beta-485044	charred material	7630 ± 40	8456 ± 81	start sedimentation	SU-3
GA-I	Beta-485043	charred material	8410 ± 30	9418 ± 98	active sedimentation	SU-2
GA-I	Beta-378613[a]	charred material	8800 ± 40	9900 ± 220	age overestimation	SU-2
GA-I	Beta-404760	charred material	8460 ± 30	9488 ± 38	active sedimentation	SU-2
GA-I	Beta-499012	charred material	8230 ± 50	9215 ± 186	active sedimentation	SU-2
GA-II	Beta-485036	charred material	4170 ± 30	4698 ± 123	start colluviation	SU-7
GA-II	Beta-499008	charred material	4320 ± 30	4902 ± 62	stagnant sedimentation	SU-6
GA-II	Beta-486033	charred material	5090 ± 40	5831 ± 88	active sedimentation	SU-5
GA-II	Beta-485029	charred material	5400 ± 30	6204 ± 83	stagnant formation	SU-4
GA-II	Beta-485028	charred material	6270 ± 30	7213 ± 53	active formation	SU-4
GA-II	Beta-485031	charred material	6660 ± 30	7533 ± 52	active formation	SU-4
GA-II	Beta-499007	charred material	7630 ± 40	8456 ± 81	stagnant sedimentation	SU-3
GA-II	Beta-485026	charred material	7620 ± 40	8442 ± 77	stagnant sedimentation	SU-3
GA-II	Beta-485027[a]	charred material	6460 ± 30	7374 ± 57	age underestimation	SU-3
GA-II	Beta-485037	charred material	8920 ± 30	10053 ± 136	active sedimentation	SU-2
GA-III	Beta-485040	charred material	5370 ± 30	6147 ± 131	stagnant formation	SU-4
GA-III	Beta-485039	charred material	6720 ± 40	7587 ± 77	start formation	SU-4
GA-III	Beta-499010	charred material	8290 ± 30	9283 ± 142	active sedimentation	SU-2
GA-IV	Beta-485041	charred material	7430 ± 30	8259 ± 74	active formation	SU-4
GA-V	NZA 61388	gastropod shell	6807 ± 33	7638 ± 48	active formation	SU-4
GA-VI	Beta-485024	charred material	4950 ± 30	5671 ± 65	active colluviation	SU-7
GA-VI	Beta-485025	charred material	4830 ± 30	5560 ± 84	active colluviation	SU-7
GA-VI	Beta-485022[a]	charred material	5900 ± 30	6724 ± 62	age overestimation	SU-6
GA-VI	Beta-485023	charred material	5230 ± 30	6045 ± 129	start sedimentation	SU-5
GA-VII	Beta-485038	charred material	9160 ± 30	10323 ± 83	start sedimentation	SU-2
GA-VIII	Beta-485035	charred material	770 ± 30	701 ± 33	active sedimentation	SU-9
GA-VIII	Beta-499009	charred material	550 ± 30	578 ± 62	active sedimentation	SU-9
GA-VIII	Beta-485034	charred material	2220 ± 30	2238 ± 86	active sedimentation	SU-8

[a] Not included into age model due to age over- or underestimation.

SU-4: A radical shift of sedimentation behavior was observed in SU-4, leading over to the formation of massive strata of paludal type tufa deposits (Pedley, 2009) with a thickness partly exceeding 5 m. In general, *in situ* formed tufa layers are characterized by a phytoherm fabric with densely packed and vertically aligned carbonate tubes (see photograph in Fig. 4D). These layers alternate with tufa layers characterized by a predominance of a microbially precipitated lime mud with admixed carbonate debris as well as rolled and partly patinated tube fragments. Moreover, numerous up to 30 cm thick grayish clay layers are interposed reflecting short periods of fine-sediment supply and deposition under presumably high-flood conditions. Carbonate contents reach values between 60 and 90 percent, depending on the admixture of silicate sediments (Fig. 5). Partly, massive iron strains can be recognized and charred plant material can be found inside the carbonate tubes. Discrete, up to five cm thick organic layers appear especially in the lower part of SU-4 (see photograph in Fig. 4C, upper part). Another peculiarity of SU-4 is the abundance of a wide variety of fossil gastropod shells in the sediments. Here, a clear dominance of aquatic species is reflected with just a small proportion of terrestrial species. A detailed analysis of gastropod associations is currently in progress.

SU-5: The upper end of the tufa unit generally consists of a dark grey clayey sediment, bearing lenses of carbonate tubes and plenty of charcoal fragments. Carbonate contents of up to 60 percent (section GA-VI, Fig. 7) indicate that calcareous marls are likely to be the main source of these deposits. However, nearly 30 percent of the clay in GA-IV consists of non-calcareous material that, together with increased organic carbon content of up to 0.8 percent, may indicate pedogenic processes. However, since none of the other sections shows comparable patterns, we do currently rather not expect severe pedogenesis in SU-5.

SU-6: This unit is up to 3 m thick and marks a further strong shift in fluvial dynamics. The loamy ochre-colored material shows clear fluvial bedding structures with a continuous appearance of dark grayish-brown lenses (see photograph in Fig. 4E, lower part) full of white carbonate fragments and secondary carbonate precipitations. Thus, SU-6 consists of typical flood loam and indicates a return to more intense fluvial sedimentation dynamics including a higher supply of sediments from the catchment slopes. In both sections, GA-II and GA-III, SU-6 ends up with a relatively well-developed palaeosoil (see photograph in Fig. 4E, middle part) as evidenced by a gradual increase in darker colors and higher organic carbon contents (~0.7 percent in GA-II, Fig. 6). In section GA-III, incorporated angular detritus may show a renewed relocation of the respective sediments (Fig. 3). An important feature is the absence of SU-6 downstream the narrow part linked to GA-III (Fig. 2) that may suggest that respective sediments have not been accumulated in that lowermost part of the Galera Valley.

SU-7: The previously described sediment succession is almost ubiquitously covered by colluvial slope deposits showing dark and light pale grey colors (see photograph in Fig. 4E, upper part) and an admixture of angular or rounded clasts. Since these deposits resulted from slope erosion processes, the thickness of SU-7 is highest in distal floodplain positions close to the foot slopes and thins out towards the center of the floodplain. Clay contents are usually around 20 percent (after decalcification) and organic carbon contents belong to the highest ones in the whole sections (Figs. 6 and 7). Both indicate the incorporation of eroded soil material from the catchment slopes. A special case is expressed in section GA-VI, where the river channel apparently cut through SU-6 and accumulated a layer rich in small gravels afterwards (Fig. 7). Between these gravels and the upper part of SU-7 at the top of the section, at least one palaeosol was developed as indicated by a dark-brown color and a gradual increase of clay and organic carbon in the upper part.

The last three units SU-8 to SU-10 belong to a younger Holocene

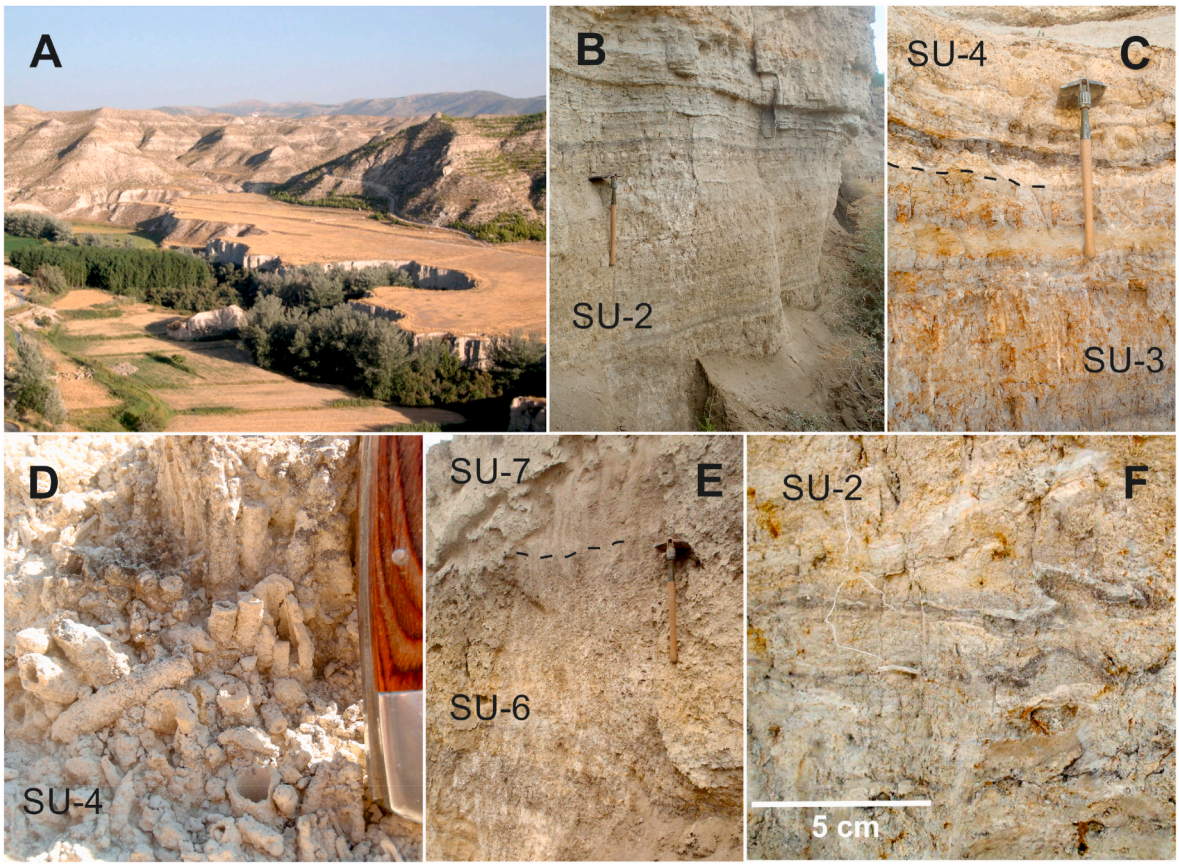

Fig. 4. Visual impressions of the Galera floodplain record. A) View of the Galera River Valley with 13 m deep incised early to mid-Holocene tufa terrace. B) Layered structure of the fluvial sediment unit SU-2 in GA-VII. c) Transition from clayey high-flood deposits of SU-3 towards calcareous tufa deposits of SU-4. Note the thin blackish layers rich in organic carbon and different iron compounds in the lower part of SU-4 (photo taken from section GA-I). D) Typical vertical arrangement of calcareous tubes in an in-situ tufa deposit (section GA-I). E) Transition of alternating sandy (ochre) and loamy (grey-brown) layers of the fluvial deposit SU-6 towards homogeneous greyish colluvial deposits of SU-7. In the uppermost part of SU-6 (spade blade), a dark humic palaeosol developed (photo taken from section GA-II). F) Small-scale folding structures in a laminated part of SU-2, presumably caused by seismic activity (section GA-I).

terrace body and were only observed in section GA-VIII (Fig. 8).

SU-8: This unit is characterized by many rounded to sub-angular gravels with diameters up to 30 cm and numerous gastropod shells and carbonate tube fragments (Fig. 8). Moreover, there are huge iron or manganese-bearing concretions with a length of up to 80 cm. Accordingly, this sediment unit must have formed in a highly dynamic fluvial regime in a former river channel. It forms the base of a younger Holocene river terrace and marks an important turnaround of river behavior leading over from incision towards accumulation.

SU-9: The overlying part of the younger Holocene terrace is composed of grayish loamy deposits in the lower half and an alternation of grayish loams and ochre-colored sand layers in the upper half (Fig. 8). The loams continuously show white and soft carbonate enrichments, while the general calcium carbonate content amounts to 40 to 50 percent.

SU-10: A dark-grey colluvial deposit with admixed rounded clasts (Fig. 8) tops the young Holocene terrace. According to recent utilization of the terrace surfaces, these colluvial deposits were mainly formed by human land-use practices and the cultivation of field terraces.

4.2. Occurrence and distribution of the early to mid-Holocene Galera 'tufa-terrace'

The particular value of the Galera floodplain record is demonstrated by a chronologically highly resolved reflection of early to mid-Holocene landscape dynamics in the central Baza Basin. In this regard, an up to 17 m thick terrace-body (see photograph, Fig. 4a) represents the most characteristic feature of this floodplain record. Apart from fluvial and colluvial sediment units, this sequence includes an up to 5 m thick unit of fluvial tufa deposits. Fluvial tufa is a calcareous deposit that precipitates from carbonate-rich waters due to physicochemical processes and the activity of in-stream cyanobacteria, mosses and algae (Pedley, 1990; Capezzuoli et al., 2014). A prerequisite for tufa formation is intense carbonate dissolution in aquifers of calcareous bedrock. In general, tufas are linked to warm and especially humid environmental conditions in Mediterranean regions (Sancho et al., 2015; Pedley, 2009).

The mapping of the fluvial tufa unit revealed that the thickest deposits appear between the towns of Galera (that is located at the confluence of the rivers Galera and Orce) and Castilléjar (that is located at the confluence of the Huéscar River in the Guardal River) (Fig. 2). Downstream Castilléjar we could not find remains of Holocene floodplain deposits forming distinct terrace levels. Upstream Galera the amount of river incision strongly decreases and the fluvial tufas seemingly run out in a huge sediment cover of the Huéscar river valley. Within the valley of the Orce River, no Holocene tufa deposits could be identified so far.

Referring to the inner structure of the tufa-terrace, the cross-sections in Fig. 9 (first and second section) show that the fluvial sediment units (SU-2 to SU-6) appear with a more or less horizontal bedding across the floodplain. However, it becomes obvious that the thickest deposits are located in the central parts of the floodplain, while deposits are thinning along the outer fringes. Moreover, the deposits are more elevated in

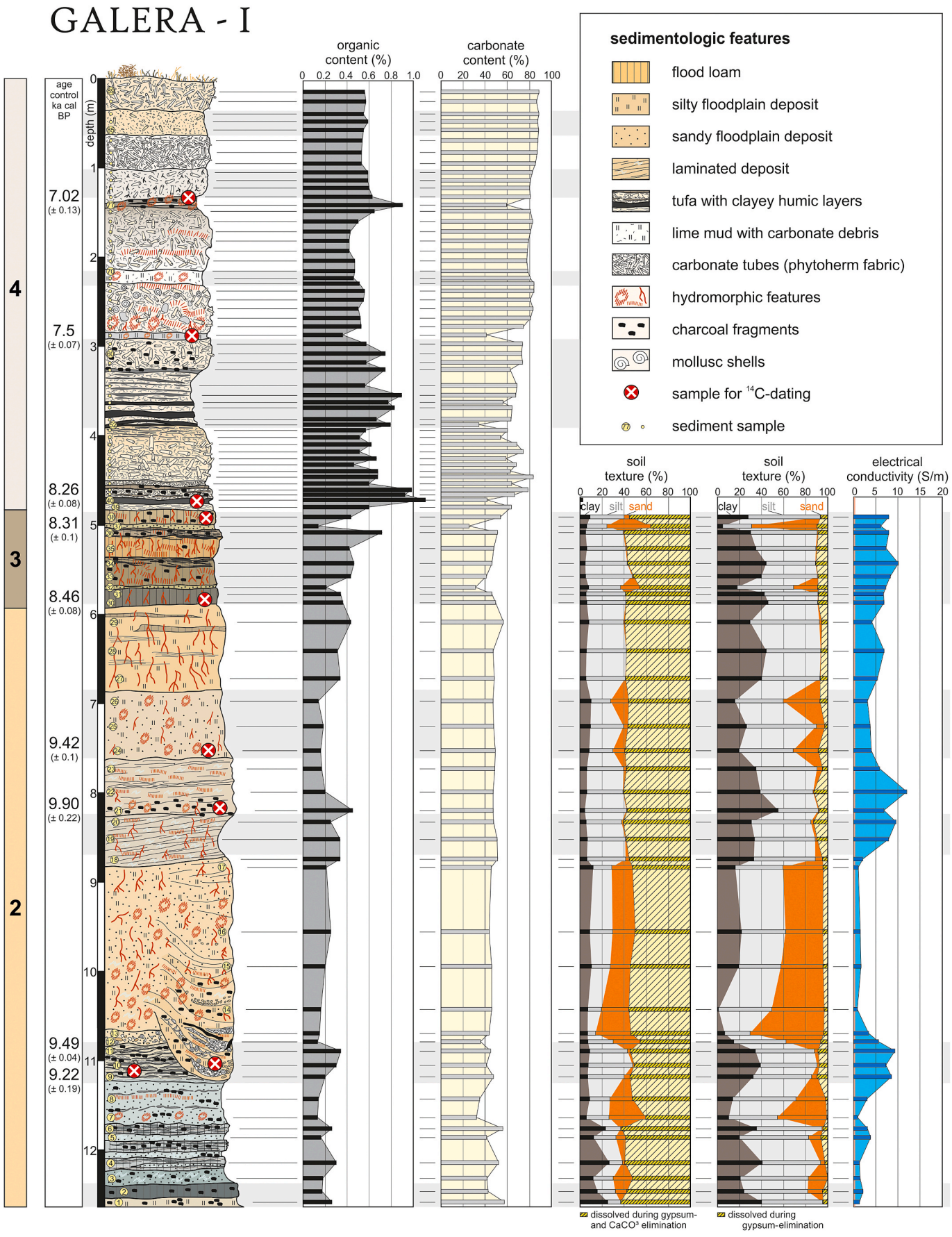

Fig. 5. Profile sketch of section GA-I with ^{14}C dating information as well as results of analytical work.

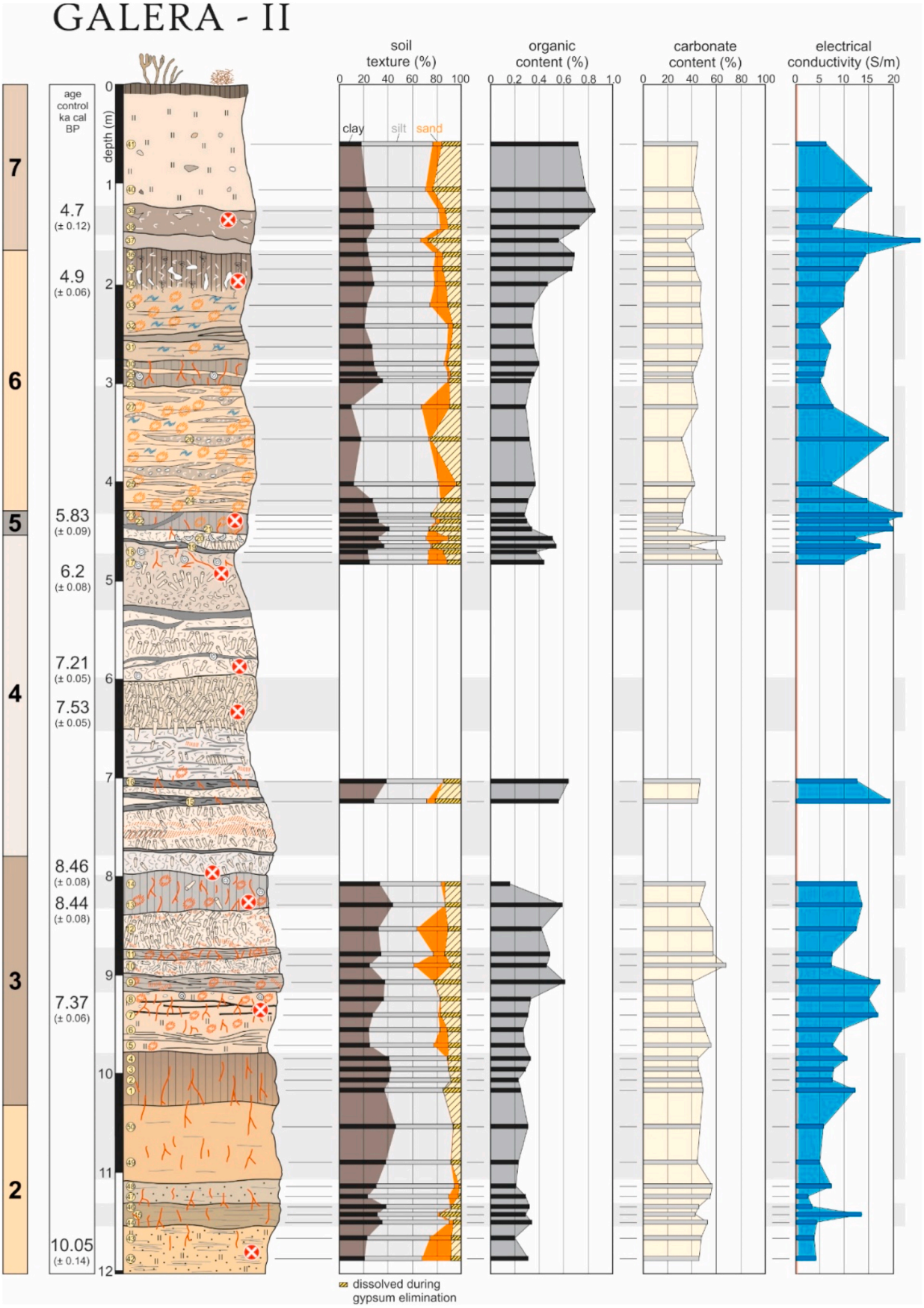

Fig. 6. Profile sketch of section GA-II with ^{14}C dating information as well as results of analytical work. For legend, see Fig. 5.

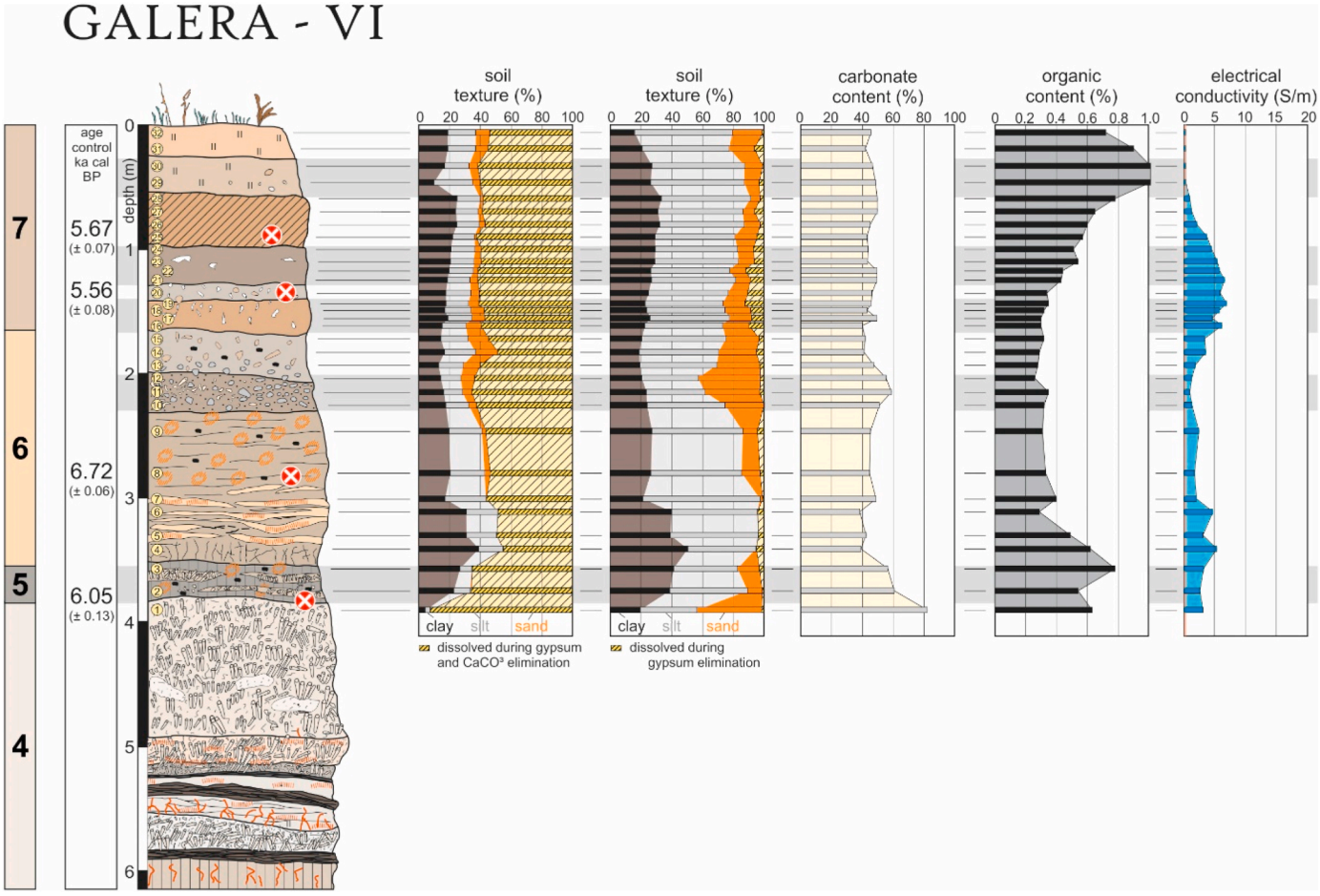

Fig. 7. Profile sketch of section GA-VI with ^{14}C dating information as well as results of analytical work. For legend, see Fig. 5.

these fringe areas leading to concave shaped valley floors instead of flat floodplain surfaces. In the outermost segments of the valley floor, the fluvial sediment units intermesh with colluvial deposits from the catchment slopes. In general, the fluvial sequences are topped by a succession of colluvial deposits (SU-7). This colluvial cover reaches a thickness of up to 7 m in peripheral foot slope positions and thins out up to a thickness of 1 m towards the floodplain center.

Another aspect relates to the appearance of the early to mid-Holocene (tufa) terrace along the Galera river course. From the town of Galera until about 500 m east of Cortijo del Cura (Fig. 2), the width of this terrace is about 250–600 m and the modern river channel is running around 16–18 m below the top of the tufa-terrace (Fig. 10) depending on the preservation state of the sediment sequences. In general, the river channel incised about 1.5–2 m into the underlying substratum, i.e. the endorheic bedrock. This means that the maximum thickness of the Holocene sequence represented by the tufa-terrace is roughly 16–17 m. In the area of Cortijo del Cura, the Holocene floodplain shows a strong narrowing. Even if the whole valley becomes up to 500 m wide, a ~20 m high erosional terrace that was carved out from the endorheic bedrock during the Pleistocene period dominates the valley floor (Fig. 9, third section). Here, the 14 m high tufa-terrace solely appears at the southern side of the valley and apparently, Holocene sedimentation dynamics were limited to a 150–200 m wide area (Fig. 10) and did not surpass the height of the erosional terrace. As show by García-Tortosa et al. (2011), the Galera fault is directly running through the Galera valley in that position (Fig. 2). Along that narrow passage, huge blocks and fallen pillars of the framing marl substratum together with blocky debris cones may testify strong tectonic activities (e.g. earthquakes) in the past. Downstream this narrow passage, the Holocene valley floor widens again (Figs. 10 and 9, fourth section) leading to a sudden increase of accommodation space that is evidenced by tufa deposits solely 5 m above the recent river channel. Here, the strongly anthropogenically terraced surface does not allow identifying different natural terrace levels. Moreover, other fluvial units above the tufa layer (SU-4) are completely missing (Fig. 3, GA-IV).

4.3. Chronological information of the Galera floodplain record

In general, plenty of charcoal was found in the sections, however, after cleaning and pretreatment of the samples, often just a very low amount of carbon was left. In a couple of cases, the material for dating was just before the critical mass limit. Anyway, 32 radiocarbon dates shown in Table 1 were

obtained. Two samples, from sections GA-I (at a depth of 8.2 m) and GA-VI (at a depth of 2.8 m) were removed due to age over-estimation as indicated by bracketing age information. Another sample from section GA-II (at a depth of 8.3 m) was removed because of a too young age (see ^{14}C-dates in Table 1).

The remaining 29 radiocarbon dates are largely consistent as illustrated in a Bayesian model in Fig. 11 that forms the basis for the temporal classification of Galera River floodplain dynamics in the same figure. According to dating results, fluvial sedimentation in the early Holocene (SU-2) took place between ~10.3 and ~8.7 ka cal BP, and was followed by the accumulation of the clayey deposits of SU-3 until ~8.3 ka cal BP. In section GA-II (Fig. 6), tufa was already formed before 8.4 ka and section GA-IV (Fig. 3) indicates tufa formation in an earlier phase, too. We interpret the synchronous formation of fine-grained high-flood deposits and incipient tufa layers as corresponding to a kind of

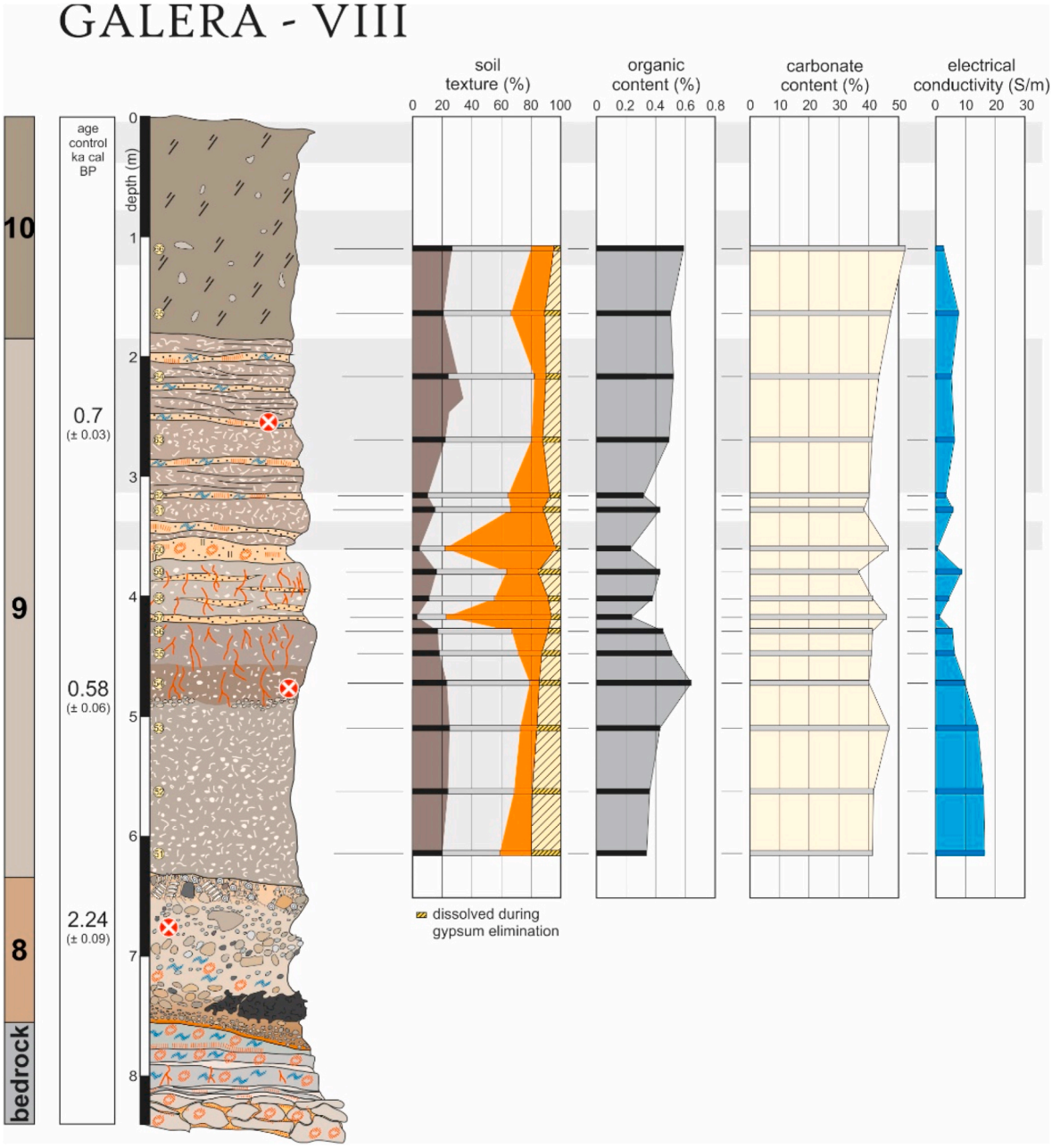

Fig. 8. Profile sketch of late Holocene section GA-VIII with ^{14}C dating information as well as results of analytical work. For legend, see Fig. 5.

transitional or stabilization phase leading over from initially highly energetic sedimentation processes towards stable surface conditions with almost absent sediment contribution from the catchment slopes. After tufa formation started latest around 8.3 ka cal BP, the built-up of the up to 5 m thick tufa sequences lasted until ~6.1 ka cal BP. The subsequent accumulation of grayish clays between ~6.1 and ~5.7 ka cal BP in SU-5 marks a further transitional phase that introduced another period of stronger fluvial sedimentation processes that started around 5.7 and ended around 4.8 ka cal BP (SU-6). The colluvial deposits on top of the sequences revealed an age of 4.7 ka cal BP, but accumulated partly already around ~5.6 ka cal BP. Here, we assume that according to the respective position within the river valley, in certain more distal places colluviation started a bit earlier, while in other places fluvial dynamics were still dominating. After 4.7 ka cal BP, no indications of fluvial sedimentation in the tufa terrace were found anymore, which suggests lacking inundation and the beginning of severe river incision presumably coeval with colluviation processes. Afterwards, the deepening of the river reached values of up to 15 m and stopped sometime before ~2.3 ka cal BP as indicated by channel deposits (SU-8) at the base of a younger Holocene sediment body (GA-VIII, Fig. 8). This more than 5 m thick sequence accumulated until ~0.7 to ~0.6 ka cal BP (SU-9) and was finally covered by another colluvial deposit (SU-10). During the youngest Holocene period, renewed river incision took place until the channel reached the underlying endorheic bedrock again.

5. Discussion

As mentioned in the introduction, archive features resulting from fluvial processes cannot always be assigned to specific causes without doubt. In case of the Galera River, we have been able to describe the chronological sequence of erosion and sedimentation phases in the previous sections. In the discussion, we will focus on possible formation processes of the sediment archive and try to identify dominant influencing factors.

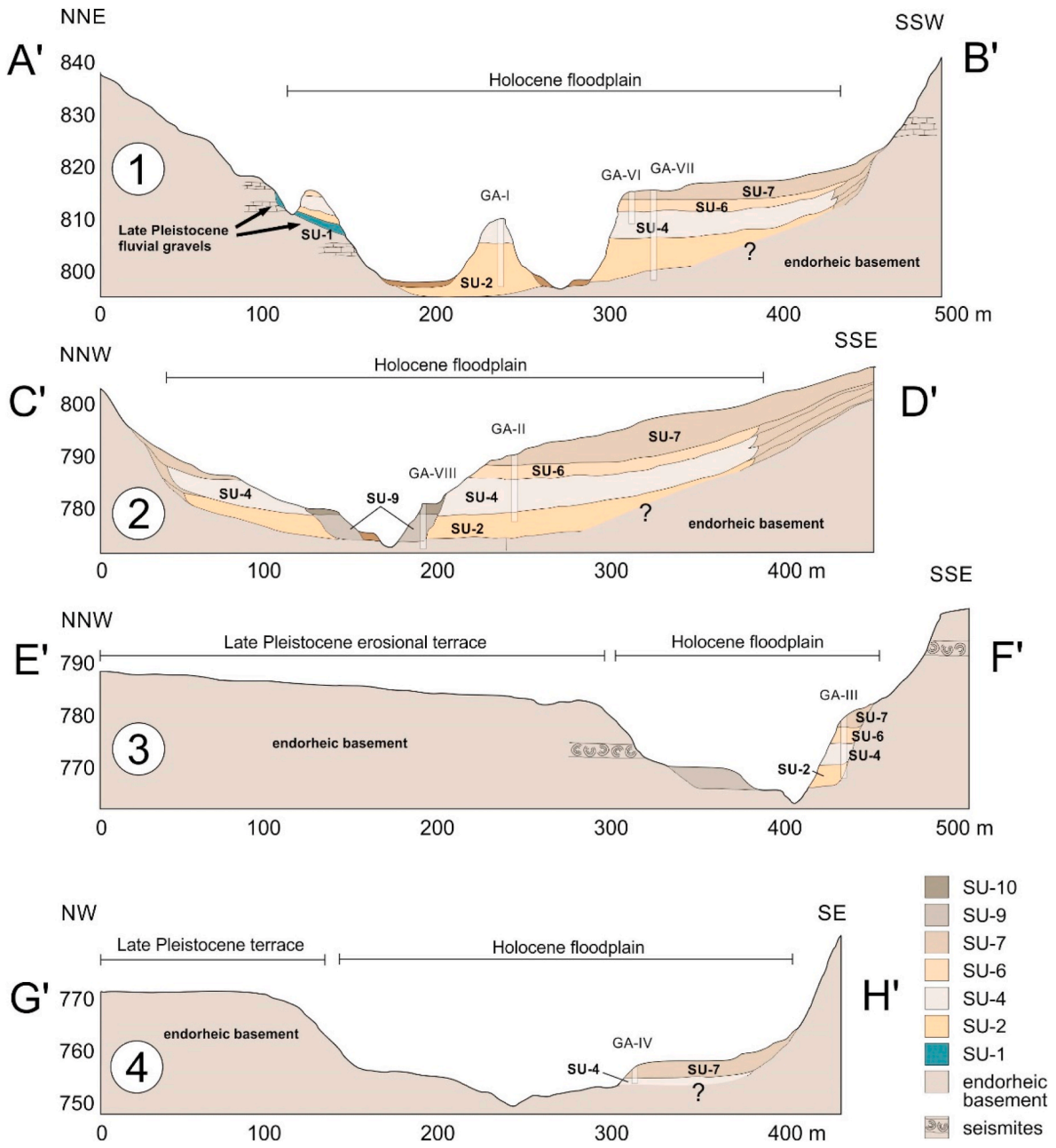

Fig. 9. Different cross-sections through the Galera Valley based on the Digital Elevation Model (DEM) of Andalucía 1:20.000 (Junta de Andalucía, 2005) and field observations. All cross-sections are indicated by letters in Fig. 2. For detailed descriptions of sediment units (SU) see section 4.

5.1. Interpretation of morphodynamics during the Holocene

5.1.1. Early Holocene river incision (11–10.3 ka)

The Early Holocene as well as the end of the last glacial period have been characterized by a strong incision phase that led to a down-cutting by assumedly more than 10 m (Fig. 9, first section). No information is available regarding the beginning of river incision, but it ended sometime before 10.3 ka cal BP when the system switched to aggradation (Fig. 11). Causes for river incision may be manifold (e.g., environmental forcing, base level lowering, tectonic uplift, etc., see Faust and Wolf, 2017), however, a general relation between incision and Pleistocene cold-stage episodes has been shown for European river systems (Gibbard and Lewin, 2009). Thus, climate changes were considered the main drivers for deep valley incision during the Pleistocene. In Iberian river systems, late Pleistocene incision often related to sea-level lowering (Schulte et al., 2008; Vis et al., 2008; Wolf et al., 2014) that is unlikely to apply to the Galera River very far from the Atlantic as ultimate base level. Nevertheless, it is a crucial question for an appropriate interpretation of Galera River behavior whether incision periods have been predominantly controlled by downstream factors (the base level of erosion, and thus the dynamics of the Guardal River) or by upstream factors (influence of climate and climatically controlled changes in discharge and sediment supply, see Blum and Törnqvist, 2000). So far, there are no information from the Guardal Valley concerning late Pleistocene and Holocene incision and aggradation periods. A study on sedimentary sequences of the Guadiana Menor that drains the GBB to the Guadalquivir Valley suggests river incision of 45–70 m within a period between 24 and 5.6 ka cal. BP (García-García et al., 2016). Considering a distance of more than 70 km between both study sites implying several crossing fault lines and knick-points in the valley gradient, as well as concomitant time lags due to regressive bed erosion (e.g. Kolb et al., 2016), a direct transferability of the results may be

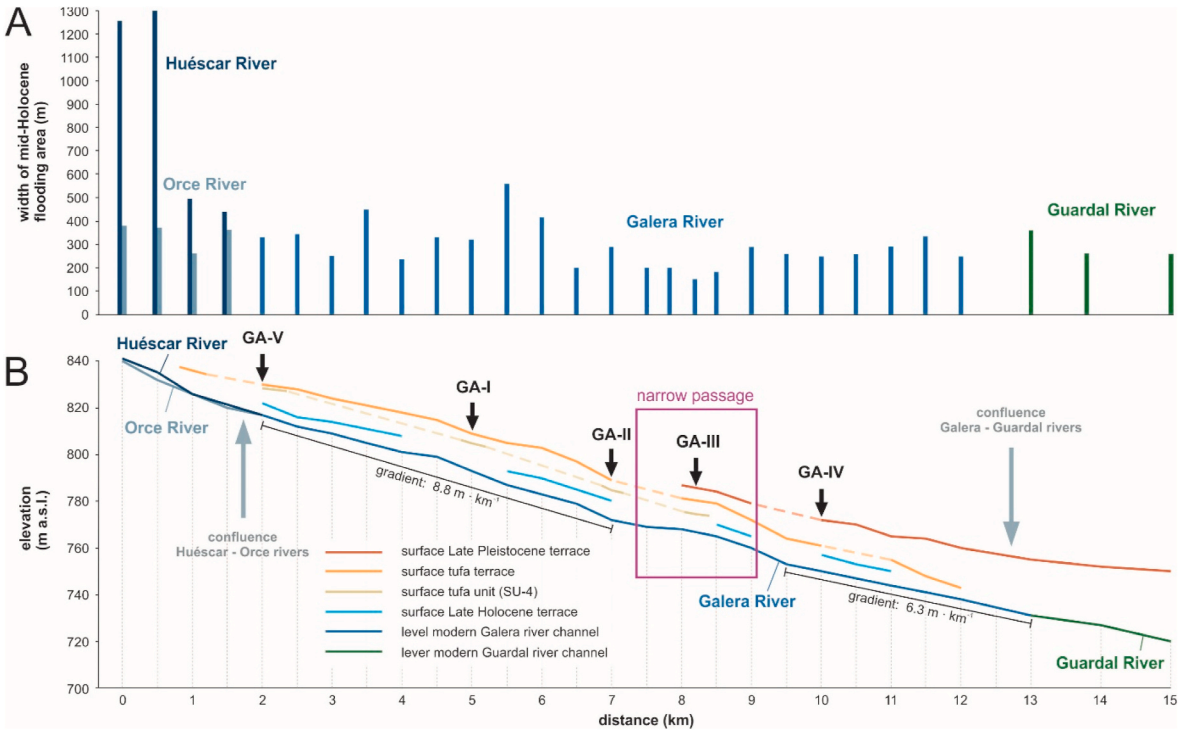

Fig. 10. Size parameters of the early to mid-Holocene terrace in the Galera Valley. A) Estimated width of the mid-Holocene flooding surface based on field-mapped extension of respective sediments in combination with DEM information (1:20.000; Junta de Andalucía, 2005). On the left side, the assumed extension of the terrace in the Huéscar river valley (dark blue) and the Orce river valley (light grey blue). On the right side, the width of the Holocene floodplain in the Guardal River (green) is visible. B) Longitudinal profiles showing the surfaces of the different late Pleistocene and Holocene terraces measured each 500 m (indicated by vertical dotted lines). Information on the surface of the tufa unit (SU-4, pale green) was directly taken from the analyzed sections. While the tufa terrace appears likewise further upstream in the Huéscar Valley (left side), no indications were found further downstream in the Guardal Valley (right side). Moreover, longitudinal river profiles and confluences of the Orce and Huéscar rivers (left side) and the Guardal River (right side) are visible. The violet square marks the narrowing of the Holocene floodplain and a knick-point in the modern river gradient.

questionable. However, we assume that large parts of the GBB drainage network may have been characterized by incision rather than aggradation during the fading Late Glacial period. Moreover, incision in the Galera Valley would not be possible without incision of the Guardal River as immediate receiving stream. Principally, river incision should be accompanied by high runoff and low sediment supply e.g., due to protecting vegetation cover in areas without permafrost (Lane, 1955; Langbein and Schumm, 1958), although fluvial reactions on climate conditions may be highly variable and depend e.g., on different catchment properties (Vandenberghe, 2003). Climate-sensitive pollen archives from the wider region suggest a generally cold and dry climate with periglacial conditions in the Segura Mountains between 20 and 12 ka cal BP (Siles; Carrión, 2002) and a late glacial warming towards Mediterranean conditions between 12 and 10 ka cal BP. Pollen data from the Alborán Sea suggest cold and arid conditions linked to a high abundance of semi-desert taxa and low arboreal pollen concentrations during MIS 2 (Fletcher et al., 2008). Pollen-based reconstructions of mean annual temperature and precipitation revealed lowest values for both parameters between 17.5 and 15 ka cal BP (Fletcher et al., 2010). This was followed by a strong increase of Mediterranean forest around 15 ka (start of Bölling-Allerød interstadial) in line with a strong increase of precipitation (Combourieu Nebout et al., 2009; Fletcher et al., 2010), increasing northern hemisphere insolation as well as decreasing global ice volume. A brief return of aridity and colder conditions was observed for the Younger Dryas (Fletcher et al., 2008). Also a $\delta^{13}C$ record of a flowstone from the Victoria Cave, ~130 km east of our study area, revealed higher precipitation between 15 and 10 ka (except for the Younger Dryas) that might have promoted denser vegetation cover in that region (Budsky et al., 2019, Fig. 12D). Riverine supply to the Western Mediterranean Sea was moderately high between 15 and 20 ka, but indicates a strong increase around 13.5 ka (Rodrigo-Gámiz et al. 2011, 2013, 2013; Martinez-Ruiz et al., 2015). From this it follows that Galera river incision took place (i) in line with strong aridity and coldness until 15 ka and during the Younger Dryas, or (ii) accompanied by increasing temperature and precipitation between 15 and ~10 ka. While the first case would indicate highest precipitation variability with high magnitude runoff events leading to erosion and bedrock incision, the latter would point towards incision due to more balanced rainfall promoting denser vegetation cover, lower catchment erosion/sediment supply, and thus a lower sediment-load-ratio.

5.1.2. *Early Holocene floodplain aggradation (10.3–8.2 ka)*

Following the incision period, river behavior experienced a major change around 10.3 ka cal BP towards massive aggradation of an interbedded sequence of silty and sandy deposits (SU-2) up to 8 m thick (Fig. 3). The interbedding indicates high sediment supply to the floodplain with frequent variations of river discharge. Channel structures testify highly intense channel dynamics, while lacking coarse-grained channel deposits may evidence a rapidly aggrading floodplain area. All these features refer to a strong change in runoff patterns during the early Holocene involving a higher runoff variability and a tendency towards more frequent flooding events. This, together with a higher erosion efficiency due to opened vegetation cover points to a lower frequency of more intense precipitation events that, in turn, may suggest a dryer climate and an increased seasonality. This interpretation is in good agreement with isotope records of Victoria cave (Budsky et al., 2019, Fig. 12D) as well as a higher proportion of xerophytic vegetation in the Segura Mountains (Siles, Villaverde and Cañada records) (Carrión et al. 2001, 2010; Carrión, 2002) (Fig. 12B). In a wider context, this might be related to higher northern hemisphere solar summer insolation

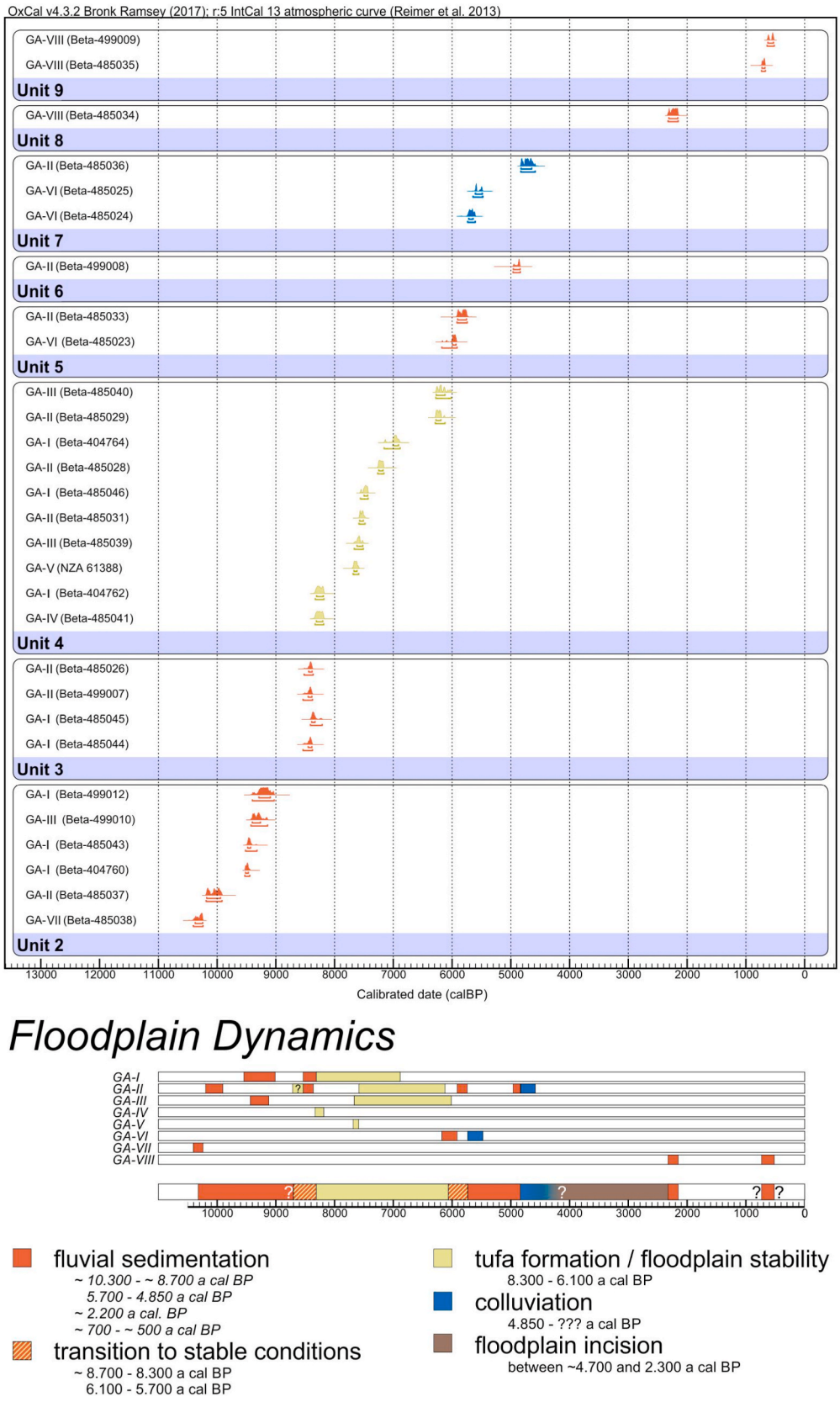

Fig. 11. All ^{14}C ages obtained from the Galera floodplain record shown in a Bayesian model. Ages are colored according to sediment units. The lower part of the figure shows the synthesis of the ages including a classification of dominating processes that took place in the Galera floodplain. These processes are shown for each section individually and as a composite in the lowermost bar.

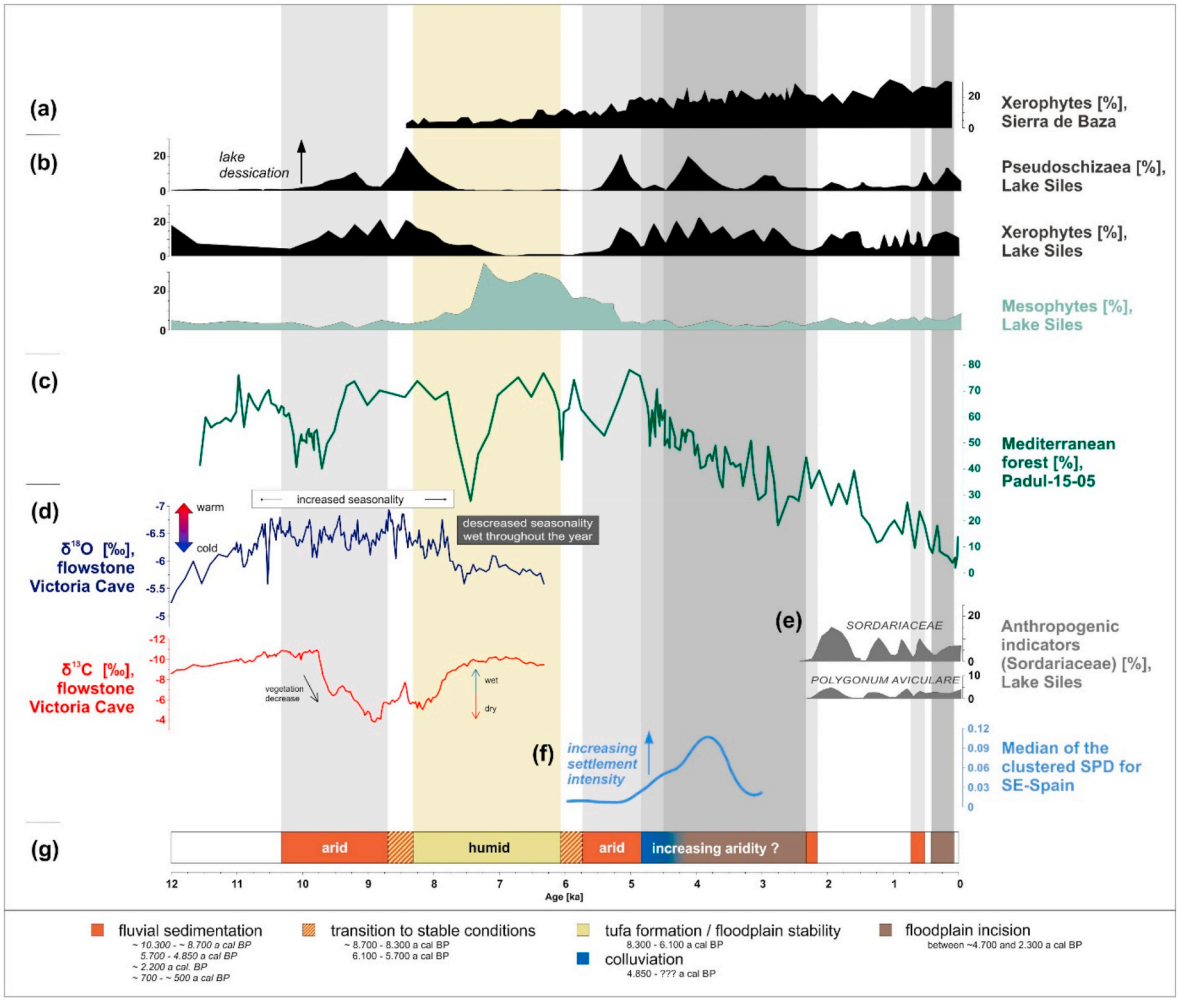

Fig. 12. Compilation of Holocene floodplain formation processes in the Galera River system as well as palaeo-climate and anthropogenic indicators from a regional context in SE-Spain, with a) pollen percentages of xerophytic vegetation detected in the Sierra de Baza (Carrión et al., 2007); b) pollen percentages of Pseudoschizaea, Xerophytes, and Mesophytes from Lake Siles (Carrión, 2002); c) pollen percentages of Mediterranean forest from Padul-15-05 (Ramos-Román et al., 2018); d) stable isotope information from a flowstone in Victoria Cave (Budsky et al., 2019); e) Pollen percentages of anthropogenic indicators from Lake Siles (Carrión, 2002); f) clustered summed probability densities (SPDs) of AMS ^{14}C dates from Copper and Bronze Age archaeological contexts in SE-Spain (Schirrmacher et al., 2020); g) sequence of Holocene floodplain dynamics as derived from Fig. 11 with main hygric information provided by sedimentation contexts. Vertical bars indicate: light grey – sedimentation, middle grey – colluviation, dark grey – incision, and light green – tufa formation.

during the early Holocene (Berger, 1978; Harrison et al., 1992). Even if charcoal is a common feature in fluvial sequences, the vast abundance of charcoal layers within SU-2 (Figs. 3 and 5) suggests a relation to increased fire dynamics during the early Holocene. In this regard, this finding is likewise consistent with a high charcoal accumulation rate in the Cañada and Siles sequences (Gil-Romera et al., 2010) pointing to a strong fire activity during a presumably dry climatic phase (Carrión, 2002). In summary, the Galera floodplain record reflects the general landscape dynamics during the early Holocene (10.3–~8.7 ka cal BP) in SE-Spain, showing that dry climate conditions and/or high seasonality led to sparse vegetation cover, intensified catchment erosion, strengthened flooding dynamics, and finally intense floodplain aggradation. As an important factor from a fluvial perspective, already the shift in precipitation distribution towards stronger seasonal patterns should have outweighed a pure decrease of annual precipitation amounts in terms of geomorphic efficiency (Eybergen and Imeson, 1989; Lavee et al., 1998; Faust and Wolf, 2017).

From ~8.7 until 8.3 ka cal BP, a transitional phase towards more stable landscape conditions is indicated by several layers of clayey deposits (SU-3) testifying reduced flow velocities at inundated floodplain areas. The almost negligible proportion of silicate sand fractions together with the high content of carbonate clays (Fig. 5) point to dominating short distance transport with the main source being the adjacent marl slopes instead of more distant areas in the catchment. This may point to a certain slowdown of sediment dynamics across the catchment due to decreasing rainfall variability and stabilizing plant cover. A plenty of charcoal fragments was found in SU-3 with black coal coatings tracing former surface levels (Fig. 5). During the same time, an early Holocene maximum in micro-charcoal occurs in all studied sequences in the Segura Mountains showing a high fire incidence contemporaneously with a desiccation event in Siles (Carrión, 2002), which suggests that fires have been climatically induced. However, the Galera record indicates a certain calming of river dynamics including incipient soil formation processes linked to surface stability (see section GA-I, Fig. 5) and an intermesh with relocated or in-situ tufa deposits (e.g. GA-II, Fig. 6). Thus, the abundance of charcoal in SU-3 might also relate to a gradual increase of fuel availability in the course of increasingly wetter climate conditions. This is supported e.g. by a serious reduction of xerophytic vegetation and a strong increase of pines and limnological indicators observed for Cañada de la Cruz (Carrión et al., 2001; Gil-Romera et al., 2010) in the Segura Mountains. Likewise in Siles, xerophytes are in decline in that period and mesophytes show a

weak first enrichment (Carrión, 2002) predicting already an end of the early Holocene aridity period.

5.1.3. Mid-Holocene tufa formation (8.3–~6 ka)

Latest at 8.3 ka cal BP another strong change of morphodynamic conditions took place that initiated continuous tufa formation testifying a high degree of landscape stability within the catchment. Thick strata of phytoherm facies characterized by cushion-like stem incrustations that developed on grasses or semi-aquatic vegetation (Fig. 4D) witness a sluggish drainage along the valley floor (see Pedley, 2009). The dominance of calcium carbonate in these layers (Fig. 5) reflects prevailing sediment retention on catchment slopes, which in turn indicates a strong expansion of forest vegetation cover (González-Amuchastegui and Serrano, 2015; Sancho et al., 2015; Aranbarri et al., 2016; Dabkowski, 2020). An increased soil CO_2 production under forest vegetation led to increased $CaCO_3$ solution in the aquifers and the discharge of chemically active groundwater (Sancho et al., 2015). Finally, tufa formed after CO_2 outgassing in the paludal system as well as CO_2 uptake through cyanobacterial photosynthesis (Arenas et al., 2014). Regarding the climatic context of tufa formation, higher water availability and warmer temperatures that support CO_2 outgassing of the river discharge suggest the prevalence of warm and humid conditions (Pedley, 2009; González-Amuchastegui and Serrano, 2015) that are typically found for the Atlantic period in Iberia. This is consistent with the so-called tufa maximum that has been documented in many different parts of the Western Mediterranean (Durán 1996 Martín-Algarraet al., 2003; Pedley, 2009; Aranbarri et al., 2016; Dabkowski, 2020). A comparison with regional climate sensitive archives shows a good agreement between tufa formations in the Galera Valley, vegetation increase in the area of Victoria cave (indicated by more negative $\delta^{13}C$-values; Budsky et al., 2019, Fig. 12D) and a replacement of xerophytes and *Pseudoschizaea* by mesophytes in Siles (Carrión, 2002) (Fig. 12B).

A closer look to Fig. 12 reveals that the beginning of tufa formation preceded the strong rise of mesophytes in Siles by around 0.8 ka, which is beyond the uncertainties of radiocarbon dating. Therefore, we expect that for different reasons the tufa system was somehow more sensitive towards incipient climate changes as compared to the vegetation system at Siles. This is even more obvious when considering that the calming of river dynamics already started at about 8.7 ka cal BP with the formation of SU-4. Tufa systems are exceptionally fragile and respond quickly to dynamic changes (Pentecost, 1995; Andrews, 2006; Dabkowski, 2014; González-Amuchastegui and Serrano, 2015). Probably, already smallest changes of runoff and discharge patterns could have initiated serious changes of river behavior in the Galera Valley, while the upper catchments especially in the mountains remained less affected. However, the proportion of xerophytes at Siles culminated already at about 8.3 ka simultaneously with the onset of tufa formation and gradually decreased until ~7.3 ka. Apparently, this gradual change in mountain areas was countered by earlier and more abrupt dynamic changes in the central Baza Basin. Perhaps, this earlier response could be linked to the different altitudes of the study sites and related precipitation patterns that led to more pronounced changes of vegetation and runoff patterns within the lower situated basin.

Additional palaeoenvironmental indications are provided by an accumulation of blackish layers rich in clay, organic material and iron compounds that were mostly formed in a period before 7.5 ka cal BP in the lower part of the tufa sequence (SU-4) (Figs. 4C and 5). Since these layers can be found in wide horizontal dimensions along the whole floodplain, we assume them to represent flooding events during which eroded surface material was accumulated in the valley floor probably following extended wildfires (see González-Amuchastegui and Serrano, 2015). A higher accumulation of charcoal particles and thus, a higher fire activity was likewise documented for Siles at 8 ka with a strong decrease around 7.5 ka, fitting very well with the increase in mesophytes and deciduous oaks in the region (Gil-Romera et al., 2010). If moreover information from Victoria cave (Budsky et al., 2019, Fig. 12B) is included, a regional palaeoenvironmental pattern emerges pointing to already moister conditions between 8.2 and 7.5 ka that were interrupted by dry spells. After 7.5 ka, the wettest conditions during the Holocene have been achieved (see e.g. Yanes et al., 2011) including strongest spread of vegetation cover, lowest fire incidence, most pronounced tufa formation in the Galera floodplain and thus, lowered seasonality.

Another question relates to the fact that no other vast meteogene tufa deposits were found in Holocene river valleys of the Baza Basin, so far. We assume that this is mainly caused by the uniqueness of the geoconstellation in the Galera river catchment area and especially the immediate study area. In particular, we assume that the geological substratum plays a dominant role here, which consists of Pliocene and Pleistocene limestone and marls (Fig. 1) that show high contents of calcite or dolomite (Gibert et al., 2007). With calcite proportions higher than 60 percent in middle Pleistocene deposits or even 79 percent in late Pliocene strata (García-Aguilar et al., 2014) these substrates appear to be effective suppliers of calcium carbonate enabling tufa formation within the incised river valley. Perhaps, the geological fracture zone linked to the Galera Fault, which runs parallel to the Galera river valley (García-Tortosa et al., 2011), contributed to the emergence of numerous springs that yielded carbonate-enriched waters to the discharge. A similar combination between bedrock-derived chemistry of spring water and the location of springs as determined by bedrock structure were identified as main factors for tufa formation in the Frailes system west of the GBB (García-García et al., 2013b).

5.1.4. Tufa decline around 6 ka and mid-Holocene floodplain aggradation (until ~4.8 ka)

According to radiocarbon dating, the formation of tufa in the Galera Valley declined abruptly around 6 ka, which is consistent with the so-called 'Late Holocene Tufa Decline' observed in Western Europe, especially in fluvial tufa (Goudie et al., 1993; Dabkowski, 2020). Two different reasons are usually given to explain such a decline: the first relates to climatic changes especially in terms of the establishment of drier conditions that abolished sedimentary environments suitable for tufa precipitation (e.g. Pedley, 2009; Domínguez-Villar et al., 2012; Aranbarri et al., 2016). The second specifies that the tufa decline was mostly driven by human activity linked to deforestation and clearance of natural systems (e.g. Pedley, 2009; González-Amuchastegui and Serrano, 2015). As a general relation, the degradation of vegetation cover on catchment slopes causes higher runoff and soil erosion. That, together with reduced biological activity, alters the soil conditions in terms of released CO_2 fluxes to the aquifers and leads to decreased calcium carbonate supply to the drainage (Dabkowski, 2020, see references within). Moreover, an increased supply of detrital material to the drainage facilitates physical erosion of tufas in the course of extreme hydrological events (Sancho et al., 2015).

However, the Galera floodplain record offers a different picture of landscape dynamics since tufas are covered by a series of different fluvial deposits without any indication of incision or erosion in between (Fig. 3). With increased organic carbon contents and very high proportions of calcium carbonate (Fig. 7), the dark grey and clayey material of SU-5 directly above the tufa sequence indicates incipient surface erosion on adjacent catchment slopes and the translocation of soil material to the floodplain. This phase took place around 6 to 5.8 ka cal BP and was partly interrupted by phases of floodplain stability as indicated by temporary tufa formation in proximal floodplain positions together with features of intense root penetration throughout SU-5 and the uppermost part of the tufa layer (SU-4) (see Fig. 3). Subsequently, the deposition of several meters of flood loam (SU-6) until ~4.9 ka cal BP evidences the return to fluvial sedimentation dynamics characterized by greater flood-frequency and a higher degree of catchment connectivity as e.g. shown by higher shares in the silicate sand fraction.

In summary, we see a "mirror" of the early Holocene units SU-2 and SU-3 and conclude that this gradual transition from stability towards higher erosion and fluvial sedimentation dynamics most likely suggests

climate forcing instead of sudden anthropogenic changes in the catchment. That means that in contrast to other Holocene tufa records on the Iberian Peninsula, where tufa decline was directly followed by incision, the fluvial sediment cover overlying the Galera tufa sequence appears to be another indication of increasing aridity between 6 and ~5 ka (see also Wolf and Faust, 2015 or Faust and Wolf, 2017). This aridification that is also clearly reflected by vegetation and fire dynamics in the Segura Mountains (Carrión, 2002; Gil-Romera et al., 2010) initiated a decrease in forest area, a decline of tufa formation and an increasing destabilization of slopes within the Galera river catchment. A climatic transition period leading over from humid conditions during the Atlantic period towards much more arid conditions after ~5.5 ka has been documented for many areas of SE-Spain and the Mediterranean region (Carrión, 2002; Carrión et al., 2003; Jalut et al., 2009; Anderson et al., 2011; Jiménez-Moreno and Anderson, 2012; Bellin et al., 2013; Lillios et al., 2016; Tarroso et al., 2016; Schirrmacher et al., 2020) (Fig. 12).

5.1.5. Colluviation and river incision during the middle to late Holocene (4.8–2.8 ka)

After flood loam deposition stopped in the Galera Valley by 4.9 to 4.7 ka cal BP, a brief phase of surface stability is indicated by the formation of a humic floodplain soil in sections GA-II and GA-III (Figs. 3 and 6). The covering colluvial deposits in GA-II point towards a sedimentation period around 4.7 ka cal BP and can be linked to slopes largely cleared of vegetation. As visible in section GA-VI, colluvial deposits date already back to 5.6 ka (Fig. 7) suggesting that processes of flood loam deposition and colluvial deposition took place simultaneously, which is not surprising since slope erosion is the main sediment supplier to floodplains. Regarding the palaeoenvironmental context, such intense colluviation processes can be interpreted as further evidence for arid conditions promoting thinning of vegetation cover and soil erosion (Eybergen and Imeson, 1989; Desprat et al., 2003; Vicente-Serrano et al., 2006; Ruiz-Sinoga and Romero Diaz, 2010). Alternatively, changes in human land-use practises or intensified agricultural activity may likewise be able to initiate vegetation clearing and soil erosion processes.

The final replacement of fluvial sedimentation by colluviation that occurred latest at 4.7 ka cal BP (Fig. 11) marks an important turnaround of river dynamics towards lacking floodplain inundation and incipient river entrenchment. Our results document a subsequent period of tremendous river incision of 15 m and partially even up to 17 m until ~2.3 ka cal BP when renewed aggradation set in. From a purely climatic perspective, fluvial incision during the Holocene is generally linked to continuous discharge with low sediment load and a high capacity of stream erosion (Lane, 1955; Wolman and Miller, 1960; Bull, 1997). This is often found for climatically favourable phases with more humid conditions promoting denser vegetation cover and sediment retention on catchment slopes (Sancho et al., 2008; Wolf et al., 2013; Sarti et al., 2015; Faust and Wolf, 2017). However, according to regional palaeoenvironmental archives in SE-Spain, this incision fell in a period of increasing aridification (Carrión, 2003; Jalut et al., 2009; Jiménez-Moreno et al., 2012; Ramos-Román et al., 2018) (Fig. 12), which strongly contradicts common concepts of climatically controlled river incision and might refer to different influencing factors. Among the causes of river incision especially tectonic impact or base level lowering are of major importance (Schumm, 1993; Blum and Törnqvist, 2000; Törnqvist, 2007; Wolf et al., 2014; Vis et al., 2010; von Suchodoletz et al., 2016; Wolf and Faust, 2016; Viveen et al., 2019; Wen et al., 2020). Furthermore, human activity may strongly alter river behavior (Hook, 2006). In order to approach a possible scenario for mid-to late Holocene river incision including the main factors that may have influenced floodplain dynamics, we will give an overview of mid-to late Holocene climate evolution, regional vegetation changes, human interventions as well as tectonic processes in section 5.2.

5.1.6. Late Holocene cut-and-fill terrace

After mid-to late Holocene river incision dissected the complete Holocene sequence, a turnaround of river behavior at about 2.3 ka cal BP (Fig. 11) led to the accumulation of a loamy gravel-bearing channel deposit (SU-8). The general change towards deposition is further illustrated by an at least 4.5 m thick sequence of loamy deposits with intercalated sand layers that was accumulated after a certain hiatus in a period around 0.6 ka cal BP. Calcium carbonate contents above 40 percent and organic contents around 0.6 percent (Fig. 8) indicate that respective sediments originated from soil erosion on adjacent marl surfaces. Palaeoenvironmental archives from the Baza Basin suggest that after a phase characterized by post-Argaric depopulation (Fig. 12F), a new push of agricultural activities set in with the Iberian culture between 3.2 and 2.2 ka. Accompanying features after 2.6 ka were forest regression, mesophyte depletion, a higher microcharcoal concentration as well as clearing activities in the mountains (Carrión et al., 2007). Apparently, this sedimentation period appears as a regional phenomenon as evidenced by aggradation in the Vinalopó Valley nearby Alicante between 2.5 and 2.4 ka (Ferrer García, 2018), in the Guadalentín Depression between 2.7 and 2.2 ka (Silva et al., 2008), in the Librilla Basin around 2.6 ka (Calmel-Avila, 2002), in the Turia Valley between 2.8 and 2.3 ka (Carmona and Ruiz, 2011) and by increased soil erosion in the Vera Basin between 2.65 and 2.15 ka (Van der Leeuw, 1998). Palaeoenvironmental archives from the region report generally more humid conditions between ~2.5 and 1.8 ka linked to the Iberian Roman Humid Period (Faust et al., 2004; Martin-Puertas et al., 2010; Jiménez-Moreno et al., 2013; Ramos-Román et al., 2016; Mesa-Fernández et al., 2018; Gázques et al., 2020) (Fig. 12C). Carrión (2002) found a strong decrease of xerophytes and microcharcoal (~2.4–2 ka) accompanied by the advent of anthropogenic indicators in the Segura Mountains (Fig. 12E), and Carmona and Ruiz (2011) link a general tendency of aggrading valley floors in that period with enhanced erosion due to human activities and expanding agriculture. Under natural conditions, more humid conditions should favour the stabilization of catchment slopes and valley floors. That means that a change from incision to aggradation in the Galera Valley around 2.3 ka could indicate a surplus of precipitation amount under still high precipitation variability entailing an increasing sediment supply to the drainage systems. Alternatively, an intensification of agricultural activities would have strongly increased sediment supply.

Likewise, the sedimentation period around 0.6 ka cal BP (SU-9) (Figs. 8 and 11) finds its analogues in different river valleys in SE-Spain (Calmel-Avila 2002, 2014, 2014; Baartman et al., 2011; Carmona and Ruiz, 2011; García-García et al., 2013a). The current chronological resolution that is solely based on one reliable date does not allow a very precise temporal classification of this sedimentation period in the Galera Valley. In the moment, we assume that it could be placed into the Little Ice Age, a period that is reflected by a sequence of catastrophic flood events and severe droughts in the region (Camuffo et al., 2003; Nieto-Moreno et al., 2011; Ramos-Román et al., 2016) especially during the 14th century (Grove, 2001; Calmel-Avila, 2014). However, since likewise human induced devastations after the Reconquista may have supported erosion and sedimentation dynamics (Calmel-Avila, 2014), the deposition of SU-9 appears to be once more a product of both climatic deterioration and human land-use changes.

5.2. Possible influencing factors for mid-to late Holocene incision of the Galera River

As derived above, tremendous river incision in a period in between 4.7 and ~2.3 ka cal BP can be related with strongly arid climate conditions. This contradicts the common concept of incision in line with humidity leading to lower sediment-load-ratios. In the following, we discuss possible scenarios for this incision against the background of regional characteristics and developments.

5.2.1. Climate development in SE-Spain

It has been frequently shown that climate appears to be a main driving force of Holocene floodplain dynamics (e.g., Macklin et al., 2012; Fletcher and Zielhofer, 2013; Wolf and Faust, 2015). In order to verify as to whether climate conditions likewise controlled mid-to late Holocene Galera river dynamics, we consulted independent climate-sensitive archive information. Most of the available information on climate development in the study region comes from palynological records that all demonstrate a strong climate change towards drier conditions between 6 and 5 ka (Carrión, 2003; Carrión et al., 2007; Jiménez-Moreno et al., 2012; Lillos et al., 2016) simultaneously with the fluvial deposition of SU-6 (Fig. 12). Very arid conditions were found after 4.6 to 4.7 ka, e.g. in the Sierra Nevada (Jiménez-Moreno et al., 2012) or in Padul (Rámos-Roman et al., 2018). For the early to mid-Holocene, Padul demonstrates continuously high percentages of Mediterranean forest (Fig. 12C) interrupted by dry spells that illustrates its position very close to the coast of the Mediterranean Sea windward to the Sierra Nevada. However, since 5 ka likewise this site experienced a strong gradual aridification until modern times. Rodríguez-Estrella et al. (2011) documented an aridity crisis in the coastal area of Murcia between 4.33 and 3.95 ka that led to the formation of a deposit of halite more than 1 m thick in a lagoon environment. According to Carrión et al. (2007), the climate change that is demonstrated e.g., by lake desiccation since 5.9 ka in the Sierra de Gador or 4.8 ka in the Sierra de Baza, clearly induced a vegetation change in the whole region. This change is evidenced by a higher incidence of xerophytes since 5.4 and 5.5 ka in the Sierras de Baza (Fig. 12A) and Gador, and finally the establishment of sclerophyllous forest at about 3.8–3.9 ka. Likewise, the fire activity intensified after 6 ka and reached a high level around 4 ka (Carrión et al., 2007; Gil-Romera et al., 2010). Apparently, this higher fire incidence that can be related to drier climate conditions, also had a strong impact on vegetation changes (Carrión, 2003; Gil-Romera et al., 2010) although a human influence on fire dynamics must be considered (Carrión, 2003; Garcia-Alix et al., 2013).

5.2.2. Anthropogenic activity in SE-Iberia

Beside climate forcing, also anthropogenic influence may strongly alter river behavior and floodplain development. This generally happens through changes in runoff patterns or sediment supply. Both may be strongly controlled by different land use practices, provided that land use intensity exceeds a certain threshold value for being reflected in landscape dynamics (Faust and Wolf, 2017). In case of SE-Iberia, there is still an open debate regarding the time at which human activities started to exercise a first serious impact on the landscape. So far, no clear evidence for Neolithic agriculture was found in SE-Spain (Carrión et al., 2007; Chapman, 2008), thus a human influence on vegetation dynamics seems improbable until 5.7 ka (Carrión, 2003). During the Copper Age that is regionally represented by the "Los Millares" culture (5.2–4.2 ka, Chapman, 2008), first evidence of metallurgy appeared (Lull, 2010) and more indications for agricultural production were found. It is expected that small settlements (<1 ha) were dominating and that a number of smaller mobile groups lived along river valleys (Lull, 2010), where they introduced dry farming along water courses (Chapman, 2008). Presumably, a versatile subsistence helped to maintain intact ecosystems (Lull, 2010) that is reflected e.g., by the absence of substantial alteration of vegetation in mountain areas (Carrión et al., 2007). After Copper Age societies entered a state of crisis around 4.5 ka (Lull, 2014), the "El Algar" culture developed in the Bronze Age between 4.2 and 3.5 ka (Lull, 2013) and soon reached the so far highest economic level in Iberia. This process related to a multiplication of the population (Castro et al., 1998; see also Fig. 12F) and an intensification of agriculture (Lull, 2013). After 3.7 ka, uniform husbandry strategies were implemented regardless of local environmental conditions. On marl surfaces, extensive dry farming was conducted, dominated by barley monocultures (Chapman, 2008) that, due to low yields and high land consumption, entailed large-scale deforestation and land clearance as well as ongoing soil degradation (Lull, 2013). Finally, the over-exploitation, perhaps in combination with increasing aridity, is assumed to have caused the Argaric collapse at 3.5 ka (Carrión et al., 2007).

For the immediate study area, a number of Argaric settlements have been documented on hilltops between Galera and Castillejar as well as east of Galera (Moreno Oronato and Haro Navarro, 2008), with the most important being Castellón Alto located 1 km upstream of GA-I section (see Fig. 2). The presence of El Argar in the Galera Valley dates back to 4.05 ka (Lull, 2014) but information on direct interactions between humans and the landscape of the Galera Valley e.g. in terms of agricultural practises are rare. According to Rodríguez-Ariza (1992), a well-developed forest composition during the Copper Age gave way to a dominance of fire-resistant *Pinus halepensis*, an indicator species for forest degradation during the Argaric period. Despite a later development towards open shrub lands, rich riparian forests in the valley bottoms were interpreted as potential conservation measures against high floods.

5.2.3. Tectonic impacts

As described above, the whole Baza Basin is a tectonically active zone. Especially the narrow steep-flanked Galera Valley that is running along a prominent fault line (Galera fault, García-Tortosa et al., 2011) (Fig. 1) is prone to tectonic influences such as seismicity and concomitant rock fall. Soft-sediment deformation in the fine laminated lower part of SU-2 (Fig. 4F) assumedly indicate the effects of seismic events on water-saturated cohesive floodplain sediments (seismites). Effects of larger dimension may have resulted from rock fall or even the collapse of whole valley flanks, while remnants of the latter are still visible in form of huge blocks and debris cones along a very narrow part of the valley (Fig. 10). Such processes may have resulted in a succession of valley damming and dissection.

5.2.4. Scenario for mid-Holocene river incision

It follows from all these considerations that the decline of tufa formation in the Galera Valley around 6 ka as well as the subsequent formation of the fluvial sediment units SU-5 and SU-6 until 4.8 ka cal BP (Fig. 11) were most probably unaffected by human activities. This strengthens our climatic interpretation of an increasing dryness that led to landscape destabilization around 6 ka and flood loam deposition afterwards. Unfortunately, we are not able to specify the time frame for the massive incision between 4.7 and 2.3 ka cal BP more precisely and it is unclear whether it started already during or even before the Argaric period. Generally, Argaric settlements were erected in elevated sheltered positions in direct proximity to cultivation areas in fertile valley bottoms (Moreno Oronato and Haro Navarro, 2008; Lull, 2010). Therefore, we assume that in the Argaric period, the Galera River was not yet strongly incised and water was still easily accessible.

Four different scenarios for mid-to late Holocene river incision in the Galera Valley can be suggested:

(1) *Incision caused by human activity*. It is uncertain whether the Argaric people actively implemented measures that influenced natural river behavior. While Capman (2008) argue the construction of water channels was a characteristic feature of husbandry during the Argaric period, Carrión et al. (2007) see no clear indications for irrigation. In turn, Rodríguez-Ariza (1992) suspect an intensive agriculture based on irrigation in such an arid zone with water control and hydraulic work by means of irrigation channels, canals, and cisterns being indispensable elements. A similar behavior is reported by Gilmann and Thornes (1985) from the Antas River catchment around 4 ka. Regarding the effects of such hydraulic measures, Huang et al. (2014) demonstrate that channel adjustments to human disturbances are predominantly expressed through channel incision and channel narrowing. Likewise channel straightening and embankment will

initiate the conversion of wide unstable river courses into single deep and narrow channels (Hooke, 2006).

However, could such irrigation measures initiate severe river incision?

The likelihood that such a channelized river will incise also depends on the sediment-load ratio and thus, the availability of sediments (Hooke, 2006). In this context Macklin et al. (2013) state, e.g., that deforestation will cause higher surface runoff, but might relate to lower sediment delivery as compared to phases of extensive ploughing of exposed soils. In view of the large catchment of the Galera River, the high utilization pressure during the Argaric period (Fig. 12F) and the increasing climate aridity (Fig. 12), it is difficult to see how sediment supply could be reduced during that period. Therefore, we assume that human activities alone would not have been able to initiate such strong river incision.

(2) *Incision caused by high-energy flooding events.* A corresponding scenario is presented by Lespez et al. (2011) who studied fluvial dynamics in the semi-desert area of Mali in West Africa. They found dramatic incision rates caused by catastrophic high-energy floods within dry events and linked this to the sudden surplus of runoff relative to sediment supply. Similarly, in the upper Segura River, García-García et al. (2013a) found a change from aggradation towards incision at ~4 ka, which they link to higher aridity that caused a torrential fluvial regime including extreme flood events leading to continuous channel deepening. As a final example, also Daniels and Knox (2005) provide a similar explanation for region-wide river incision in the semi-arid Great Plains during the last millennium. They see a strong increase of runoff related to a reduction of vegetation cover and an increased emergence of extreme flood events as the main driving factors for river incision in arid environments. However, in case of the Galera River we are doubtful regarding the significance of extreme flood events. In most parts of the Galera Valley, the incision formed a gorge within the soft floodplain deposits, not exceeding 150 m in width. We expect that highly erosive extreme flooding events would have cleared out floodplain deposits in a much wider dimension and not just along a closely confined channel belt.

(3) *Incision caused by changed runoff patterns due to climatic aridification.* As shown above, a higher sediment supply due to human activities and arid climate conditions may be compensated by high peak flows that temporarily reverse the load ratio. If, in contrast to high-energy floods, one considers a situation, in which flood flows are confined to a deepened channel-belt without the possibility to inundate floodplain areas, deep and powerful discharges would initiate bed erosion. As a result, frequent lower magnitude runoff events could lead to ongoing river incision. This incision further accelerates as soon as the incising river channel is completely detached from the floodplain converting this former floodplain into a terrace. In that way, lacking overbank flow would prevent serious sediment supply through floodplain erosion (Blum et al., 1994; Hooke, 2006; Macklin et al., 2013). A similar case is demonstrated by Blum et al. (1994) who show that frequent moderate to high-magnitude floods in the upper Colorado River catchment in North America initiated late Holocene floodplain aggradation. In contrast, river incision and floodplain abandonment took place in the course of decreased flood magnitudes following a shift towards drier climatic conditions. However, since generally aridification comes along with increasing rainfall variability and magnitude of runoff events, such a scenario would imply that utmost aridity led to an attenuation of the discharge peaks.

(4) *Incision caused by tectonic impacts.* A conceivable scenario linked to tectonic activity would be that large parts of the framing soft rocks collapsed after seismic shaking and dammed the whole valley floor. This may have led to a blocking effect and a subsequent flattening of the river gradient further upstream. For instance, García-García et al. (2013b) document a similar relationship between valley-damming and tufa formation for the Frailes tufa, although in a Pleistocene context. We do not expect that such a damming was the main cause for tufa formation in the Galera Valley, because these tufa deposits represent a clear climate signal. Moreover, we found tufa likewise downstream the position of the potential damming (section GA-IV, Figs. 3 and 10), which indicates tufa formation all along the valley. However, as visible in Fig. 10, flood loams of SU-6 run out in the range of the narrow passage close by Cortijo del Cura and we found no indication of these sediments further downstream. Fig. 10 likewise demonstrates that this narrow passage is linked to a general knickpoint in the modern Galera River gradient (gradient of 8.8 $m \cdot km^{-1}$ upstream and 6.3 $m \cdot km^{-1}$ downstream) and a local flattening and steepening in form of a convex bulging. Perhaps, this configuration marks the concurrence of very solid rocks of the endorheic basement, and tectonic movements along the Galera fault, that together with landslides of rock boulders may have produced a temporarily effective barrier. In such a case, SU-6 might represent a prograding backfilling that would be expectable behind such a valley damming. A subsequent gradual cutting through the barrier would mean a base level lowering and could initiate far-reaching incision into the upstream sedimentary infill.

In summary, we found some hints that tectonic impacts may have influenced floodplain dynamics especially along the narrow passage at Cortijo del Cura (Figs. 2 and 9), however, such relations are very difficult to prove. Furthermore, there are no information on aggradation and incision dynamics from the receiving Guardal River that defines the base level for Galera River dynamics. But what we see is that the river incised during a long-lasting period of climatic aridity (Fig. 12). The first part of this arid period was still characterized by floodplain aggradation, while around 4.8 ka floodplain aggradation ceased and the valley bottom stabilized. We assume that this tipping point was controlled by an increased aridity that, in contrast to the common view that increasing rainfall variability implies increasing flood magnitudes, led to decreasing peak-flows and finally less frequent low-magnitude runoff events. At a certain point, a further threshold crossing took place and the river started to incise. At present, it is hardly possible to find out the real trigger for the onset of incision. On the one hand, a tectonically related valley damming and downstream increase of the flow velocity may have initiated incision and back cutting of the river. This may have been additionally reinforced by the narrowness of this valley section that led to a more concentrated water flow (jet effect) (Figs. 9 and 10). Perhaps, already the general constriction of the valley width at the confluence of the huge Huéscar floodplain into the narrow Galera floodplain (Fig. 10) was associated with a more erosive discharge, especially since the majority of sediments should have been deposited upstream this bottleneck. On the other hand, human activities e.g. in form of flow concentration measures may have reinforced the natural erosive power that emanated from the changed discharge patterns. Anyway, we assume that mid-to late Holocene incision of the Galera River was rather caused by a combination of different factors instead of only one (see also Huang et al., 2014). Regarding the consequences of river incision for anthropogenic utilization purposes Huang et al. (2014) emphasise the negative effects of a lower ground water table as well as a lower level of stream flow, that finally makes gravity flow water extraction for irrigation impossible. We can just assume that the apparently earlier abandonment of Castellón Alto at about 3.65 ka BP (Lull, 2013) and thus ~200 years earlier than other Argaric settlements may have been related to an

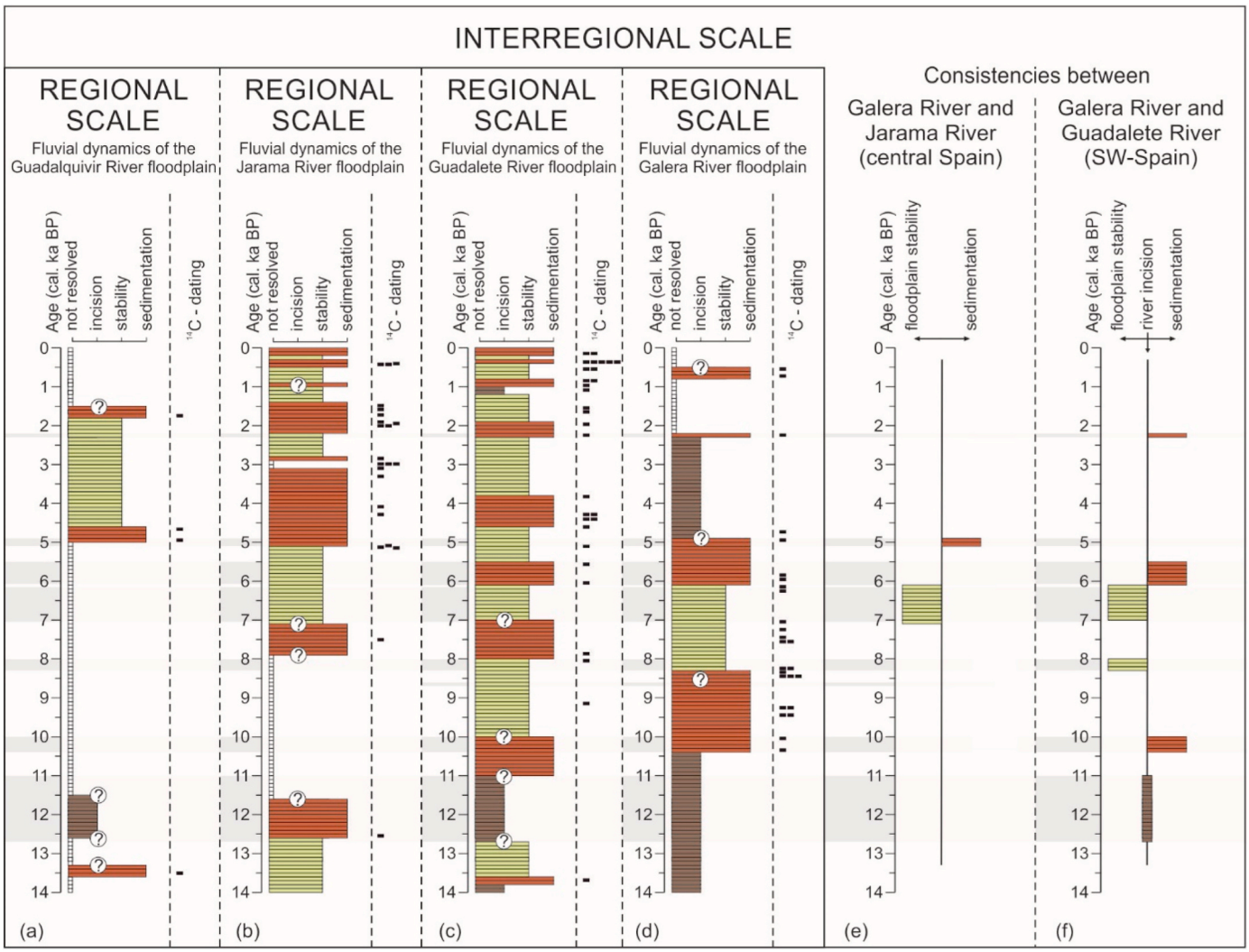

Fig. 13. Summary of late Pleistocene and Holocene floodplain dynamics of a) the Guadalquivir River in SW-Spain, b) The Jarama River in central Spain, c) the Guadalete River in SW-Spain, and d) the Galera River in SE-Spain. Furthermore, phases are indicated, when similar floodplain dynamics (stability – green; sedimentation – red; incision - black) overlap in the Galera and the Jarama systems (e), as well as the Galera and the Guadalete systems (f). The comparison between Galera and Jarama river dynamics reveals rather inconsistencies, apart from a short time span between 7 and 5 ka, while the comparison between Galera and Guadalete River dynamics reveals a slightly higher degree of consistency, especially during the early to mid-Holocene. However, since 5.5 ka floodplain dynamics strongly deviate again. Data of a), b), and c) are taken from Wolf and Faust (2015).

advanced incision state of the Galera River.

5.3. Fluvial dynamics of the Galera River in an Iberian context

A comparison between fluvial dynamics of the Galera River and further Atlantic influenced river systems in Iberia (Jarama River in central Spain; Guadalete River in SW Spain; Guadalquivir River in SW Spain; Wolf and Faust, 2015) shows just a low degree of similarity in terms of sedimentation, incision, or stability periods. As visible in Fig. 13, certain conformities exist between the Galera and Guadalete rivers, both situated in Andalucía. River incision overlap between ~12.7 and ~11 ka contemporaneous with the cold and arid Younger Dryas, albeit sea level lowering also strongly controlled incision in the Guadalete system. Fluvial sedimentation was found in both systems during the early Holocene (~10 ka) that, in each system, could be linked to arid climate conditions. The same applies to sedimentation periods after 6 ka and around 2.3 ka (Wolf et al., 2014; Wolf and Faust, 2015).

Apparently, floodplain stability without serious flooding dynamics have been a common feature in Iberia around 7 to 6 ka pointing to supra-regional landscape stability on the Iberian Peninsula during the Atlantic period. All other periods reveal rather differences than similarities (Fig. 13). Between 8 and 7 ka, stability in the Galera system was accompanied by sedimentation in the Atlantic influenced part of Iberia. During the phase of strong river incision in the Galera Valley in a period after 5 ka, all other river systems, including the Guadalquivir River, revealed floodplain sedimentation (Fig. 13). For the youngest part of the Holocene, the resolution of dynamic patterns is very low for the Galera system, but so far, there are barely any similarities.

Our compilation of palaeoenvironmental information in Fig. 12 shows that Galera floodplain dynamics during the early and middle Holocene were apparently strongly influenced by the general climatic evolution in the region. However, likewise in the other river systems, fluvial dynamics were primarily controlled by climate conditions (Wolf and Faust, 2015). Therefore, the lack of similarities between fluvial dynamic patterns of the Galera River and the other studied rivers in Iberia may allow following conclusions to be drawn:

(1) The current climate situation is different between the compared river systems with lower mean annual precipitation in the Galera system and stronger seasonal differences due to a higher altitude

and continentality. Also in former periods of the Holocene, climate conditions have been partly different, that may explain deviating patterns of fluvial dynamics.

(2) An even more striking finding is that deviating fluvial dynamic patterns resulted from a different reaction of the river systems despite seemingly similar climatic conditions. These different reactions can be attributed to a strong imprint of local to regional non-climatic factors such as tectonic activity, relief configuration, the character of the geological substratum, or human land use practices. For example, between 7 and ~6 ka, the Jarama and Guadalete river systems were characterized by floodplain stability and soil formation. As a rule, morphodynamically stable phases are more likely to be accompanied by river incision due to a lower load-ratio and higher transport capacity. However, these relations were not reflected in the Galera Valley, where the whole valley floor underwent tufa formation during a morphodynamic stable phase that led to the built-up of an up to 5 m thick tufa sequence (Fig. 11) due to the occurrence of calcareous bedrock in and around the Baza Basin (Fig. 1). As discussed above, we assume that similar to soil formation in the other river systems likewise this tufa formation was dominantly controlled by humid and warm climatic conditions. This finally means an illustrative example that the same causes (humid conditions) may lead to different process regimes and sedimentary features (Faust and Wolf, 2017), also known as the divergence phenomenon (Schumm, 1991; Philipps, 2014).

Considerable dichotomy is likewise reflected by river dynamics after 5 ka. While the circum-Mediterranean aridification around 5 ka (Jalut et al., 2009; Roberts et al., 2011) caused serious floodplain aggradation in the Guadalete and Jarama river systems (as well as in the Guadalquivir as the final receiving stream to the Galera River, Wolf and Faust, 2015), the response of the Galera system was heavy incision (Fig. 11). Here we provided a scenario that might explain river incision under very arid conditions due to moderated precipitation events, attenuated runoff peaks, reduced sediment supply, and a higher capacity of streambed erosion. Additionally, we found major influence of tectonics and relief configuration, and possibly human interventions. However, we clearly see that fluvial dynamics are not just a simple reflection of the climatic configuration. Instead, a number of different factors that especially arise from different catchment characteristics influence river behavior and floodplain dynamics. Of course, this hampers a straightforward interpretation of fluvial dynamic features without deeper knowledge of all the physical conditions of a catchment area. But it further extents the potential range of river and floodplain responses to a wide variety of mutually reinforcing factors, and thus enables an even more detailed reconstruction of palaeoenvironmental conditions and landscape evolution.

6. Conclusions

We compiled a detailed stratigraphic floodplain record for the Galera river system within the Baza Basin in SE-Spain. Our results demonstrate that river behavior and floodplain dynamics experienced several strong changes during the Holocene that enable a detailed reconstruction of landscape evolution in the region. After the Galera River incised about 10 m into older gravel and endorheic bedrock during the late Pleistocene/early Holocene, several meters of sandy to loamy deposits accumulated until ~8.7 ka evidencing unstable landscape conditions during an early Holocene aridity period. Following a transitional stabilization phase, catchment stability under warm and humid climatic conditions initiated the formation of a thick tufa sequence between 8.3 and ~6 ka during the Atlantic period. At 6 ka, tufa formation declined and gave way to another phase of highly dynamic fluvial sedimentation that we interpret as an evidence for increasing destabilization of catchment slopes in line with the mid-Holocene circum-Mediterranean aridification. After flood loam deposition stopped at 4.8 ka, the floodplain was dominated by the accumulation of colluvial slope deposits indicating a further increase of aridity. A strong turnaround of river behavior took place between 4.7 and 2.3 ka, when the river incised deeply into its sediments until it reached the endorheic bedrock again. Other archive information point to ongoing environmental aridification during that time. Since common concepts of fluvial geomorphology fail to explain such a scenario, we provide an explanation that invokes a general lowering of flood magnitudes and sediment supply to the drainage system as main causes for river incision under arid climate conditions. However, we also assume a major impact of non-climatic factors such as tectonics, relief configuration, and human activities during the Argaric period for triggering the river's decoupling from active floodplain processes. River incision turned into floodplain aggradation after 2.3 ka again, while a thick fluvial sediment body was accumulated around 0.6 ka ago, simultaneously with climatic deterioration during the Little Ice Age. For this late Holocene period, we expect that fluvial aggradation was linked to a combination of highly variable extreme flood events and increased land-use pressure due to the expansion of agriculture.

A closer look to regional palaeoenvironmental archives shows that Galera river dynamics followed a trend of climate development during the Holocene period. However, certain dynamics such as the middle to late Holocene incision seem to be controlled by catchment-specific factors like geological substrate or specific land-use measures. A comparison of Galera river dynamics with other river systems in central and SW-Iberia reveals a rather low level of conformity of fluvial dynamic patterns. This was partly caused by deviating palaeo-climatic conditions. However, in case of similar climate situations, we suggest that deviating fluvial reactions (also referred to as divergence phenomenon) mainly resulted from an additional imprint of catchment-specific factors. This shows that specific fluvial dynamics generally reflect climate and environmental conditions within a river catchment, but if different catchments are compared, these relations may not be straightforward because the imprint of catchment-specific factors may even lead to opposite geomorphological patterns. This should be considered when interpreting floodplain records, especially in the Mediterranean region.

Declaration of competing interest

The authors declare that they have no known competing financial interests or personal relationships that could have appeared to influence the work reported in this paper.

Acknowledgements

We greatly acknowledge the German Research Foundation (DFG) for funding this project (FA 239/22-1 and FA 239/24-1). Moreover, we thank the Spanish Ministry of Science, Innovation and Universities for funding (TASCUB - RTI2018-100737-B-I00). We thank B. Winkler and S. Gerstenhauer (Technische Universität Dresden) for lab work, and F. Schneider (Georg-August-Universität Göttingen) and P. Baumgart for assistance with fieldwork. Furthermore, we would like to thank J. I. Santisteban (Complutense University of Madrid) and J. Vázquez-Navarro (Universidad Autónoma de Madrid) for fruitful discussions in the field. Open Access Funding by the Publication Fund of the TU Dresden.

References

AEMET, 2011. Atlas Climático ibérico/Iberian Climate Atlas. Agencia Estatal de Meteorología (AEMET), Madrid, Spain.

Alfaro, P., Delgado, J., Sanz de Galdeano, C., Galindo-Zaldívar, J., García-Tortosa, F.J., López-Garrido, A.C., López-Casado, C., Marín-Lechado, C., Gil, A., Borque, M.J., 2007. The Baza Fault: a major active extensional fault in the central Betic Cordillera (south Spain). Int. J. Earth Sci. 97, 1353–1365.

Anderson, R.S., Jiménez-Moreno, G., Carrión, J.S., Pérez-Martínez, C., 2011. Postglacial history of alpine vegetation, fire, and climate from Laguna de Río Seco, Sierra Nevada, southern Spain. Quat. Sci. Rev. 30, 1615–1629.

Andrews, J.E., 2006. Paleoclimatic records from stable isotopes in riverine tufas: synthesis and review. Earth Sci. Rev. 17, 85–104.
Antoine, P., Lautridou, J.P., Laurent, M., 2000. Long-term fluvial archives in NW France: response of the Seine and Somme rivers to tectonic movements, climate variations and sea-level changes. Geomorphology 33, 183–207.
Aranbarri, J., Bartolomé, M., Alcolea, M., Sancho, C., Celant, A., González-Sampériz, P., Arenas, C., Magri, D., Rodríguez-Lázaro, J., 2016. Palaeobotanical insights from early-mid Holocene fluvial tufas in the Moncayo Natural Park (Iberian Range, NE Spain): regional correlations and biogeographic implications. Rev. Palaeobot. Palynol. 234 (Suppl. C), 31–43.
Arenas, C., Vázquez-Urbez, M., Auqué, L., Sancho, C., Osácar, C., Pardo, G., 2014. Intrinsic and extrinsic controls of spatial and temporal variations in modern fluvial tufa sedimentation: a thirteen-year record from a semi-arid environment. Sedimentology 61, 90–132.
Baartman, J.E.M., Veldkamp, A., Schoorl, J.M., Wallinga, J., Cammeraat, L.H., 2011. Unravelling late Pleistocene and Holocene landscape dynamics: the upper guadalentin basin, SE Spain. Geomorphology 125, 172–185.
Bellin, N., Vanacker, V., vanWesemael, B., Sole-Benet, A., Bakker, M.M., 2011. Natural and anthropogenic controls on soil erosion in the internal Betic Cordillera (southeast Spain). Catena 87, 190–200.
Bellin, N., Vanacker, V., De Baets, S., 2013. Anthropogenic and climatic impact on Holocene sediment dynamics in SE Spain: a review. Quat. Int. 308, 112–129.
Benito, G., Thorndycraft, V., Rico, M., Sánchez-Moya, Y., Sopeña, A., 2008. Palaeoflood and floodplain records from Spain: evidence for long-term climate variability and environmental changes. Geomorphology 101, 68–77.
Berger, A., 1978. Long-term variations of daily insolation and Quaternary climate changes. J. Atmos. Sci. 35, 2362–2367.
Blum, M.D., Törnqvist, T.E., 2000. Fluvial responses to climate and sea-level change: a review and look forward. Sedimentology 47, 2–48.
Blum, M.D., Toomey III., R.S., Valastro Jr., S., 1994. Fluvial response to late quaternary climatic and environmental change, edwards plateau, Texas. Palaeogeogr. Palaeoclimatol. Palaeoecol. 108, 1–21.
Bronk Ramsey, C., 2009. Bayesian analysis of radiocarbon dates. Radiocarbon 51, 337–360.
Budsky, A., Scholz, D., Wassenburg, J.A., et al., 2019. Speleothem δ13C record suggests enhanced spring/summer drought in south-eastern Spain between 9.7 and 7.8 ka – a circum-Western Mediterranean anomaly? Holocene 29, 1113–1133.
Bull, L.J., 1997. Magnitude and variation in the contribution of bank erosion to the suspended sediment load of the River Severn, UK. Earth Surf. Process. Landforms 22, 1109–1123.
Calmel-Avila, M., 2002. The Librilla "rambla" an example of morphogenetic crisis in the Holocene (Murcia, SE Spain). Quat. Int. 93–94, 101–108.
Calmel-Avila, M., 2014. Le petit age de glace (PAG) dans la vallée du Guadalentín (Sud-Est de l'Espagne, region de Murcie. Méditerranée 122, 113–119.
Camuffo, D., Sturaro, G., Benito, G., 2003. An opposite flood pattern teleconnection between the Tagus (Iberian Peninsula) and Tiber (Italy) rivers during the last 1000 years. In: Thorndycraft, V.R., Benito, G., Barriendos, M., Llasat, M.C. (Eds.), Palaeofloods and Climatic Variability: Applications in Flood Risk Management. CSICCCM, Madrid, pp. 295–300.
Capezzuoli, E., Gandin, A., Pedley, M., 2014. Decoding tufa and travertine (fresh water carbonates) in the sedimentary record: The state of the art. Sedimentology 61, 1–21.
Carmona, P., Ruiz, J.M., 2011. Historical morphogenesis of the Turia River coastal flood plain in the Mediterranean littoral of Spain. Catena 86, 139–149.
Carrión, J.S., 2002. Patterns and processes of Late Quaternary environmental change in a montane region of southwestern Europe. Quat. Sci. Rev. 21, 2047–2066.
Carrión, J.S., Munuera, M., Navarro, C., Burjachs, F., Dupré, M., Walker, M.J., 1999. The palaeoecological potential of pollen records in caves: the case of Mediterranean Spain. Quat. Sci. Rev. 18, 1061–1073.
Carrión, J.S., Andrade, A., Bennett, K.D., Navarro, C., Munuera, M., 2001. Crossing forest thresholds: inertia and collapse in a Holocene sequence from south-central Spain. Holocene 11, 635–653.
Carrión, J.S., Sánchez-Gómez, P., Mota, J.F., Yll, E.I., Chaín, C., 2003. Fire and grazing are contingent on the Holocene vegetation dynamics of Sierra de Gádor, southern Spain. Holocene 13, 839–849.
Carrión, J.S., Fuentes, N., González-Sampériz, P., Quirante, L.S., Finlayson, J.C., Fernandez, S., Andrade, A., 2007. Holocene environmental change in a montane region of southern Europe with a long history of human settlement. Quat. Sci. Rev. 26, 1455–1475.
Carrión, J.S., Fernández, S., González-Sampériz, P., Gil-Romera, G., Badal, E., Carrión-Marco, Y., López-Merino, L., López-Sáez, J.A., Burjachs, F., 2010. Expected trends and surprises in the lateglacial and Holocene vegetation history of the iberian Peninsula and balearic islands. Rev. Palaeobot. Palynol. 162, 458–475.
Carrión, J.S., Fernández, S., Jiménez-Moreno, G., Fauquette, S., Gil-Romera, G., González-Sampériz, P., Finlayson, C., 2010. The historical origins of aridity and vegetation degradation in southeastern Spain. J. Arid Environ. 74, 731–736.
Castro, P.V., Chapman, R.W., Gili, S., Lull, V., Micó, R., Rihuete, C., et al., 1998. Aguas Project. Palaeoclimatic reconstruction and the dynamics of human settlement and land use in the area of the middle Aguas (Almería) in the south-east of the Iberian Peninsula. European Commission, Luxembourg.
Gil-Romera, G., Carrión, J.S., Pausas, J.G., Sevilla-Callejo, M., Lamb, H.F., Fernández, S., Burjachs, F., 2010. Holocene fire activity and vegetation response in South-Eastern Iberia. Quat. Sci. Rev. 29, 1082–1092.
Chapman, R., 2008. Producing inequalities: regional sequences in later prehistoricsouthern Spain. World Prehistory 21, 195–260.
Combourieu Nebout, N., Peyron, O., Dormoy, I., Desprat, S., Beaudouin, C., Kotthoff, U., Marret, F., 2009. Rapid climatic variability in the west Mediterranean during the last 25 000 years from high resolution pollen data. Clim. Past 5, 503–521.
Dabkowski, J., 2014. High potential of calcareous tufas for integrative multidisciplinary studies and prospects for archaeology in Europe. J. Archaeol. Sci. 52, 72–83.
Dabkowski, J., 2020. The late-Holocene tufa decline in Europe: myth or reality? Quat. Sci. Rev. 230, 106141.
Daniels, J.M., Knox, J.C., 2005. Alluvial stratigraphic evidence for channel incision during the medieval warm period, central great Plains, USA. Holocene 15, 736–747.
Desprat, S., Sánchez Goñi, M.F., Loutre, M.-F., 2003. Revealing climatic variability of the last three millennia in northwestern Iberia using pollen influx data. Earth Planet Sci. Lett. 213, 63–78.
Domínguez-Villar, D., Vázquez-Navarro, J.A., Carrasco, R.M., 2012. Mid-Holocene erosive episodes in tufa deposits from Trabaque Canyon, central Spain, as a result of abrupt arid climate transitions. Geomorphology 161–162, 15–25.
Eybergen, F.A., Imeson, A.C., 1989. Geomorphological processes and climatic change. Catena 16, 307–319.
Faust, D., Wolf, D., 2017. Interpreting drivers of change in fluvial archives of the Western Mediterranean - a critical view. Earth Sci. Rev. 174, 53–83.
Faust, D., Zielhofer, C., Baena, R., Diaz del Olmo, F., 2004. High resolution fluvial record of late Holocene geomorphic changes in Northern Tunisia: climatic or human impact? Quat. Sci. Rev. 23, 1757–1775.
Ferrer García, C., 2018. Dinámica fluvial durante el inicio del Holoceno superior en el curso medio del Vinalopó (Alicante, España). Bol. Geol. Min. 129, 305–330.
Fletcher, W.J., Sánchez Goñi, M.F., 2008. Orbital- and sub-orbital-scale climate impacts on vegetation of the western Mediterranean basin over the last 48,000 yr. Quat. Res. 70, 451–464.
Fletcher, W.J., Sanchez Goñi, M.F., Peyron, O., Dormoy, I., 2010. Abrupt climate changes of the last deglaciation detected in a Western Mediterranean forest record. Clim. Past 6, 245–264.
Frenkel, H., Gerstl, Z., van de Veen, J.R., 1986. Determination of gypsum and cation exchange capacity in arid soils by a resin method. Geoderma 39, 67–77.
Garcia-Aguilar, J.M., Guerra-Marchán, A., Serrano, F., Palmqvist, P., Flores-Moya, A., Martinez-Navarro, B., 2014. Hydrothermal activity and its paleoecological implications in the latest Miocene and middle Pleistocene lacustrine environments of the Baza Basin (betic Cordillera, SE Spain). Quat. Sci. Rev. 96, 204–221.
García-Alix, A., Jimenez-Espejo, F.J., Lozano, J.A., Jiménez-Moreno, G., Martínez-Ruiz, F., García Sanjuan, L., Aranda Jiménez, G., García Alfonso, E., Ruiz-Puertas, G., ScottAnderson, R., 2013. Anthropogenic impact and lead pollution throughout the Holocene in southern Iberia. Sci. Total Environ. 449, 451–460.
García-García, F., Bohorquez, P., Martínez-Sanchez, C., Perez-Valera, F., Perez-Valera, L. A., Calero, J.A., Sánchez-Gómez, M., 2013a. Stratigraphic architecture and alluvial geoarchaeology of an ephemeral fluvial infilling: climatic versus anthropogenic factors controlling the Holocene fluvial evolution in southeastern Spain drylands. Catena 104, 272–279.
García-García, F., Pla-Pueyo, S., Nieto, L.M., Viseras, C., 2013b. Sedimentology ofgeomorphologically controlled Quaternary tufas in a valley in southern Spain. Facies. https://doi.org/10.1007/s10347-013-0361-5.
García-García, F., Calero, J., Pérez-Valera, F., 2016. Morphological, pedological, and sedimentary evolution on the fringe of the southwestern European drylands during the late Pleistocene and Holocene: evidence of climate and land use changes. Catena143 128–139.
García-Tortosa, F.J., Alfaro, P., Galindo Zaldívar, J., Gibert, L., López Garrido, A.C., Sanz de Galdeano, C., Ureña, M., 2008. Geomorphologic evidence of the active Baza Fault (betic Cordillera, south Spain). Geomorphology 97, 374–391.
García-Tortosa, F.J., Alfaro, P., Sanz de Galdeano, C., Galindo-Zaldívar, J., 2011. Glacis geometry as a geomorphic marker of recent tectonics: the Guadix-Baza basin (South Spain). Geomorphology 125, 517–529.
Gázques, F., Bauska, T.K., Comas-Bru, L., Ghaleb, B., Calaforra, J.-M., Hodell, D.A., 2020. The potential of gypsum speleothems for paleoclimatology: application to the Iberian Roman Humid Period. Sci. Rep 10, 14705.
Gibbard, P.L., Lewin, J., 2009. River incision and terrace formation in the Late Cenozoic of Europe. Tectonophysics 474, 41–55.
Gibert, L., Scott, G., Martin, R., Gibert, J., 2007. The early to middle Pleistocene boundary in the Baza Basin (Spain). Quat. Sci. Rev. 26, 2067–2089.
Gilman, A., Thornes, J.B., 1985. Land Use and Prehistory in South East Spain. George Allen and Unwin, London.
González-Amuchastegui, M.J., Serrano, E., 2015. Tufa buildups, landscape evolution and human impact during the Holocene in the Upper Ebro Basin. Quat. Int. 364, 54–64.
Goudie, A.S., Viles, H.A., Pentecost, A., 1993. The late- Holocene tufa decline in Europe. The Holocene 3, 181–186.
Grove, A.T., 2001. The "Little ice age" and its geomorphological consequences in mediterranean Europe. Climate Change 48, 121–136.
Haberland, C., Gibert, L., Jurado, M.J., Stiller, M., Baumann-Wilke, M., Scott, G., Mertz, D.F., 2017. Architecture and tectono-stratigraphic evolution of the intramontane Baza Basin (Bétics, SE-Spain): constraints from seismic imaging. Tectonophysics 709, 69–84.
Harrison, S.P., Prentice, I.C., Bartlein, P.J., 1992. Influence of insolation and glaciation on atmospheric circulation in the North Atlantic sector: implications of general circulation model experiments for the Late Quaternary climatology of Europe. Quat. Sci. Rev. 11, 283–300.
Hidalgo-Muñoz, J., Argüeso, D., Gámiz-Fortis, S., Esteban-Parra, M., Castro-Díez, Y., 2011. Trends of extreme precipitation and associated synoptic patterns over the southern Iberian Peninsula. J. Hydrol 409, 497–511.
Hooke, J.M., 2006. Human impacts on fluvial systems in the Mediterranean region. Geomorphology 79, 311–335.

Huang, M.-W., Liao, J.-J., Pan, Y.-W., Cheng, M.-H., 2014. Rapic channelization and incision into soft bedrock induced by human activity - implications from the Bachang River in Taiwan. Eng. Geol. 177, 10–24.
Jalut, G., Dedoubat, J.J., Fontugne, M., Otto, T., 2009. Holocene circum-Mediterranean vegetation changes: climate forcing and human impact. Quat. Int. 200, 4–18.
Jiménez-Moreno, G., Anderson, R.S., 2012. Holocene vegetation and climate change recorded in alpine bog sediments from the Borreguilles de la Virgen, Sierra Nevada, southern Spain. Quat. Res. 77, 44–53.
Jiménez-Moreno, G., García-Alix, A., Hernández-Corbalán, M.D., Anderson, R.S., Delgado-Huertas, A., 2013. Vegetation, fire, climate and human disturbance history in the southwestern Mediterranean area during the late Holocene. Quat. Res. 79, 110–122.
Kolb, T., Fuchs, M., Zöller, L., 2016. Deciphering fluvial landscape evolution by luminescence dating of river terrace formation: a case study from Northern Bavaria, Germany. Zeitschrift für Geomorphologie, Supplementary Issues 60, 29–48.
Lane, E.W., 1955. Design of stable channels. American Society of Civil Engineers Transactions 120, 1234–1279.
Langbein, W.B., Schumm, S.A., 1958. Yield of sediment in relation to mean annual precipitation. Trans. Am. Geophys. Union 39, 1076–1084.
Lavee, H., Imeson, A.C., Sarah, P., 1998. The impact of climate change on geomorphology and desertification along a mediterranean-arid transect. Land Degrad. Dev. 9, 407–422.
Lespez, L., Le Drezen, Y., Garnier, A., Rasse, A., Eichhorn, B., Ozainne, S., Ballouche, A., Neumann, K., Huysecom, E., 2011. High-resolution fluvial records of Holocene environmental changes in the sahel: the yamé riverat Ounjougou (Mali, west Africa). Quat. Sci. Rev. 30, 737–756.
Lillios, K.T., Blanco-González, A., Drake, B.L., López-Sáez, J.A., 2016. Mid-late Holocene climate, demography, and cultural dynamics in Iberia: a multi-proxy approach. Quat. Sci. Rev. 135, 138–153.
Lull, V., Micó, R., Rihuete, C., Risch, R., 2010. Metal y relaciones sociales de producción durante el III y II milenio ANE en el sudeste de la Península Ibérica. Trab. Prehist. 67, 323–347.
Lull, V., Micó, R., Rihuete, C., Risch, R., 2013. Political collapse and social change at the end of El Argar. In: Meller, H., Bertemes, F., Bork, H.-R., Risch, R. (Eds.), 1600 – Cultural Change in the Shadow of the Thera Eruption? Landesmuseum für Vorgeschichte, Halle, pp. 283–302.
Lull, V., Micó, R., Rihuete, C., Risch, R., 2014. The La Bastida fortification system: new light and new questions on the Early Bronze Age societies in the Western Mediterranean. Antiquity 88, 395–410.
Macklin, M.G., Lewin, J., Woodward, J.C., 2012. The fluvial record of climate change. Philosophical Transactions of the Royal Society A 370, 2143–2172.
Martín-Algarra, A., Martín-Martín, M., Andreo, B., Julià, R., González-Gómez, C., 2003. Sedimentary patterns in perched spring travertines near Granada (Spain) as indicators of the paleohydrological and paleoclimatological evolution of a karst massif. Sediment. Geol. 161, 217–228.
Martín-Puertas, C., Jiménez-Espejo, F., Martínez-Ruiz, F., Nieto-Moreno, V., Rodrigo, M., Mata, M.P., Valero-Garcés, B.L., 2010. Late Holocene climate variability in the southwestern Mediterranean region: an integrated marine and terrestrial geochemical approach. Clim. Past 6, 807–816.
Martínez-Cortizas, A., Costa-Casais, M., López-Sáez, J.A., 2009. Environmental change in NW Iberia between 7000 and 500 cal BC. Quat. Int. 200, 77–89.
Martinez-Ruiz, F., Kastner, M., Gallego-Torres, D., Rodrigo-Gámiz, M., Nieto-Moreno, V., Ortega-Huertas, M., 2015. Paleoclimate and paleoceanography over the past 20,000 yr in the Mediterranean Sea Basins as indicated by sediment elemental proxies. Quat. Sci. Rev. 107, 25–46.
Mesa-Fernández, J.M., Jiménez-Moreno, G., Rodrigo-Gámiz, M., García-Alix, A., Jiménez-Espejo, F.J., Martínez-Ruiz, F., Anderson, R.S., Camuera, J., Ramos-Román, M.J., 2018. Vegetation and geochemical responses to Holocene rapid climate change in the Sierra Nevada (southeastern Iberia): the Laguna Hondera record. Clim. Past 14, 1687–1706.
Morellón, M., Aranbarri, J., Moreno, A., González-Sampériz, P., Valero-Garcés, B.L., 2018. Early Holocene humidity patterns in the Iberian Peninsula reconstructed from lake, pollen and speleothem records. Quat. Sci. Rev. 181, 1–18.
Moreno Oronato, M.A., Haro Navarro, M., 2008. Castellón Alto (Galera, Granada). Puesta en valor de un yacimiento argárico, vol. 18. Cuadernos de Prehistoria de la Universidad de Granada, pp. 371–395.
Nadal-Romero, E., García-Ruiz, J.M., 2018. Rethinking spatial and temporal variability of erosion in badlands. In: Badlands Dynamics in a Context of Global Change. Elsevier, pp. 217–253.
Nieto-Moreno, V., Martínez-Ruiz, F., Giralt, S., Jiménez -Espejo, F., Gallego-Torres, D., Rodrigo-Gámiz, M., García -Orellana, J., Ortega-Huertas, M., de Lange, G.J., 2011. Tracking climate variability in the Western Mediterranean during the LateHolocene: a multiproxy approach. Clim. Past 7, 1395–1414.
Oms, O., Anadón, P., Agustí, J., Julià, R., 2011. Geology and chronology of the continental Pleistocene archeological and paleontological sites of the Orce area (Baza basin, Spain). Quat. Int. 243, 33–43.
Ortiz, J.E., Torres, T., Julia, R., Delgado, A., Llamas, F.J., Soler, V., Delgado, J., 2004. Numerical dating algorithms of amino acid racemization ratios from continental ostracodes. Application to the Guadix-Baza Basin (southern Spain). Quat. Sci. Rev. 23, 717–730.
Pedley, H.M., 1990. Classification and environmental models of cool freshwater tufas. Sediment. Geol. 68, 143–154.
Pedley, M., 2009. Tufas and travertines of the Mediterranean region: a testing ground for freshwater carbonate concepts and developments. Sedimentology 56, 221–246.
Peña, J.A., 1985. La depresión de Guadix-Baza. Estud. Geol. 41, 33–46.
Pentecost, A., 1995. The Quaternary travertine deposits of Europe and Asia Minor. Quat. Sci. Rev. 14, 1005–1028.
Pérez-Obiol, R., Jalut, G., Julià, R., Pèlachs, A., Iriarte, M.J., Otto, T., Hernández-Beloqui, B., 2011. Mid-Holocene vegetation and climatic history of the Iberian Peninsula. Holocene 21, 75–93.
Pérez-Peña, J.V., Azañón, J.M., Azor, A., Tuccemei, P., Della Seta, M., Soligo, M., 2009. Quaternary landscape evolution and erosion rates for an intramontane Neogene basin (Guadix-Baza basin, SE Spain). Geomorphology 106, 206–218.
Phillips, J.D., 2014. Thresholds, mode switching, and emergent equilibrium in geomorphic systems. Earth Surf. Process. Landforms 39, 1096–9837.
Prado-Pérez, A.J., Hueras, A.D., Crespo, M.T., Martín Sánchez, A., Pérez Del Villar, L., 2013. Late Pleistocene and Holocene mid-latitude palaeoclimatic and palaeoenvironmental reconstruction: an approach based on the isotopic record from a travertine formation in the guadix-baza basin, Spain. Geol. Mag. 150, 602–625.
Queralt, S., Hernández, E., Barriopedro, D., Gallego, D., Ribera, P., Casanova, C., 2009. North Atlantic Oscillation influence and weather types associated with winter total and extreme precipitation events in Spain. Atmos. Res. 94, 675–683.
Ramos-Román, M.J., Jiménez-Moreno, G., Anderson, R.S., García-Alix, A., Toney, J.L., Jiménez-Espejo, F.J., Carrión, J.S., 2016. Centennial-scale vegetation and north Atlantic Oscillation changes during the late Holocene in the southern Iberia. Quat. Sci. Rev. 143, 84–95.
Ramos-Román, M.J., Jiménez-Moreno, G., Camuera, J., García-Alix, A., Anderson, R.S., Jiménez-Espejo, F.J., Carrión, J.S., 2018. Holocene climate aridification trend and human impact interrupted by millennial- and centennial-scale climate fluctuations from a new sedimentary record from Padul (Sierra Nevada, southern Iberian Peninsula). Clim. Past 14, 117–137.
Reimer, P.J., Bard, E., Bayliss, A., Beck, J.W., Blackwell, P.G., Bronk Ramsey, C., Grootes, P.M., Guilderson, T.P., Haflidason, H., Hajdas, I., Hatté, C., Heaton, T.J., Hoffmann, D.L., Hogg, A.G., Hughen, K.A., Kaiser, K.F., Kromer, B., Manning, S.W., Niu, M., Reimer, R.W., Richards, D.A., Scott, E.M., Southon, J.R., Staff, R.A., Turney, C.S.M., van der Plicht, J., 2013. IntCal13 and Marine13 radiocarbon age calibration curves 0-50,000 Years cal BP. Radiocarbon 55, 1869–1887.
Roberts, N., Brayshaw, D., Kuzucuoglu, C., Perez, R., Sadori, L., 2011. The mid-Holocene climatic transition in the Mediterranean: causes and consequences. Holocene 21, 3–13.
Rodrigo-Gámiz, M., Martínez-Ruiz, F., Jiménez-Espejo, F.J., Gallego-Torres, D., Nieto-Moreno, V., Romero, O., Ariztegui, D., 2011. Impact of climate variability in the western Mediterranean during the last 20,000 years: oceanic and atmospheric responses. Quat. Sci. Rev. 30, 2018–2034.
Rodrigo-Gámiz, M., Martinez-Ruiz, F., Rodríguez-Tovar, F.J., Jiménez-Espejo, F.J., Pardo-Igúzquiza, E., 2014. Millennial- to centennial-scale climate periodicities and forcing mechanisms in the westernmost Mediterranean for the past 20,000yr. Quat. Res. 81, 78–93.
Rodríguez-Ariza, M.O., 1992. Human-plant Relationships during the Copper and Bronze Age in the Baza and Guadix Basins (Granada, Spain), vol. 139. Bulletin de la Société Botanique de la France, pp. 451–464. Actualités botaniques (2-3-4).
Rodríguez-Estrella, T., Navarro, F., Ros, M., Carrión, J.S., Atenza, J., 2011. Holocene morphogenesis along a tectonically instable coastline in the Western Mediterranean (SE Spain). Quat. Int. 243, 231–248.
Ruiz-Sinoga, J.D., Romero Diaz, A., 2010. Soil degradation factors along a Mediterranean pluviometric gradient in Southern Spain. Geomorphology 118, 359–368.
Sancho, C., Peña, J., Muñoz, A., Benito, G., McDonald, E., Rhodes, E., Longares, L., 2008. Holocene alluvial morphopedosedimentary record and environmental changes in the Bardenas Reales Natural Park (NE Spain). Catena 73, 225–238.
Sancho, C., Arenas, C., Vázquez-Urbez, M., Pardo, G., Lozano, M.V., Peña-Monné, J.L., Hellstrom, J., Ortiz, J.E., Osácar, M.C., Auqué, L., Torres, T., 2015. Climatic implications of the Quaternary fluvial tufa record in the NE Iberian Peninsula over the last 500 ka. Quat. Res. 84, 398–414.
Sarti, G., Rossi, V., Amorosi, A., Bini, M., Giacomelli, S., Pappalardo, M., Ribecai, C., Ribolini, A., Sammartino, I., 2015. Climatic signature of two Mid-Late Holocene fluvial incisions formed under sea-level highstand conditions (Pisa coastal plain, NW Tuscany, Italy). Palaeogeogr. Palaeoclimatol. Palaeoecol. 424, 183–195.
Schirrmacher, J., Kneisel, J., Knitter, D., Hamer, W., Hinz, M., Schneider, R.R., Weinelt, M., 2020. Spatial patterns of temperature, precipitation, and settlement dynamics on the iberian Peninsula during the chalcolithic and the Bronze age. Quat. Sci. Rev. 233, 106220.
Schlichting, E., Blume, H.-P., Stahr, K., 1995. Bodenkundliches Praktikum — Eine Einführung in pedologisches Arbeiten für Ökologen, insbesondere Land- und Forstwirte und für Geowissenschaftler. 2. neubearbeitete Auflage. Blackwell Wissenschafts-Verlag, Berlin, Wien, p. 295.
Schulte, L., 2002. Climatic and human influence on river systems and glacier fluctuations in southeast Spain since the Last Glacial Maximum. Quat. Int. 93–94, 85–100.
Schumm, S.A., 1991. To interprete the earth. Ten ways to be wrong. Cambridge University Press, 133pp.
Schumm, S.A., 1993. River response to base level change: implications for sequence stratigraphy. J. Geol. 101, 279–294.
Scott, G.R., Gibert, l., Gibert, J., 2007. Magnetostratigraphy of the Orce region (Baza Basin), SE Spain: new chronologies for early plistocene faunas and hominid occupation sites. Quat. Sci. Rev. 26, 415–435.
Silva, P.G., Bardají, T., Calmel-Avila, M., Goy, J.L., Zazo, C., 2008. Transition from alluvial to fluvial systems in the Guadalentín depression (SE Spain) during the Holocene: lorca fan versus Guadalentín river. Geomorphology 100, 140–153.
Tarroso, P., Carrión, J., Dorado-Valiño, M., Queiroz, P., Santos, L., Valdeolmillos-Rodríguez, A., Célio Alves, P., Brito, J.C., Cheddadi, R., 2016. Spatial climate dynamics in the iberian Peninsula since 15 000 yr BP. Clim. Past 12, 1137–1149.

Törnqvist, T.E., 2007. Fluvial environments /Responses to rapid environmental change. In: Elias, S.A. (Ed.), Encyclopedia of Quaternary Science. Elsevier, Amsterdam, pp. 686–694.
Torri, D., Calzolari, C., Rodolfi, G., 2000. Badlands in changing environments: An introduction. Catena 40, 119–125.
Van der Leeuw, S.E., 1998. Understanding the Natural and Anthropogenic Causes of Soil Degradation and Desertification in the Mediterranean Basin. The Archaeomedes Project. Synthesis. (Chapter 5): Environmental Dynamics in the Vera Basin. reportFinal Report on Contract EV5V-CT91-0021.
Vandenberghe, J., 2003. Climate forcing of fluvial system development: an evolution of ideas. Quat. Sci. Rev. 22, 2053–2060.
Vicente-Serrano, S.M., Cuadrat-Prats, J.M., Romo, A., 2006. Aridity influence on vegetation patterns in the middle Ebro Valley (Spain): evaluation by means of AVHRR images and climate interpolation techniques. J. Arid Environ. 66, 353–375.
Vis, G.-J., Kasse, C., Vandenberghe, J., 2008. Late Pleistocene and Holocene palaeogeography of the Lower Tagus Valley (Portugal): effects of relative sea level, valley morphology and sediment supply. Quat. Sci. Rev. 27, 1682–1709.
Vis, G.-J., Bohncke, S.J.P., Schneider, H., Kasse, C., Coenraads-Nederveen, S., Zuurbier, K., Rozema, J., 2010. Holocene flooding history of the Lower Tagus Valley (Portugal). J. Quat. Sci. 25, 1222–1238.
Viveen, W., Zevallos-Valdivia, L., Sanjurjo-Sanchez, J., 2019. The influence of centennial-scale variations in the South American summer monsoon and base-level fall on Holocene fluvial systems in the Peruvian Andes. Global Planet. Change 176, 1–22.
von Suchodoletz, H., Gärtner, A., Hoth, S., Umlauft, J., Sukhishvili, L., Faust, D., 2016. Late Pleistocene river migrations in response to thrust belt advance and sediment-flux steering — The Kura River (southern Caucasus). Geomorphology 266, 53–65.
Wen, P., Wang, N., Wang, Y., Huang, Y., Cheng, H., He, T., 2020. Fluvial incision caused irreversible environmental degradation of an ancient city in the Mu Us Desert, China. Quat. Res. 1–13.
Wolf, D., Faust, D., 2015. Western Mediterranean environmental changes: evidences from fluvial archives. Quat. Sci. Rev. 122, 30–50.
Wolf, D., Faust, D., 2016. River braiding caused by rapid floodplain deformation - insights from Holocene dynamics of the Jarama River in Central Spain. Quat. Int. 407, 126–139.
Wolf, D., Seim, A., Diaz del Olmo, F., Faust, D., 2013. Late quaternary fluvial dynamics of the Jarama river in central Spain. Quat. Int. 302, 20–41.
Wolf, D., Seim, A., Faust, D., 2014. Fluvial system response to external forcing and human impact - late Pleistocene and Holocene fluvial dynamics of the lower Guadalete River in western Andalucía (Spain). Boreas 43, 422–449.
Wolman, M.G., Miller, J.P., 1960. Magnitude and frequency of forces in geomorphic processes. J. Geol. 68, 54–74.
Yanes, Y., Romanek, C.S., Molina, F., Cámara, J.A., Delgado, A., 2011. Holocene paleoenvironment (7,200-4,000 cal. years BP) of the Los Castillejos archaeological site (southern Spain) as inferred from stable isotopes of land snail shells. Quat. Int. 244, 67–75.